



# Hydrodynamic modeling of dam breach floods for predicting downstream inundation scenarios using integrated approach of satellite data, unmanned aerial vehicles (UAVs), and Google Earth Engine (GEE)

Kishanlal Darji<sup>1</sup> · Dhruvesh Patel<sup>1</sup> · Indra Prakash<sup>2</sup> · Hamad Ahmed Altuwaijri<sup>3</sup>

Received: 3 April 2024 / Accepted: 28 July 2024 / Published online: 6 August 2024  
© The Author(s) 2024, corrected publication 2024

## Abstract

Dam breach floods pose significant threats to downstream areas, necessitating accurate prediction of inundation scenarios to mitigate potential damage. This paper presents a novel methodology for hydrodynamic modeling of dam breach floods, leveraging a comprehensive approach that integrates satellite imagery, unmanned aerial vehicles (UAVs), and Google Earth Engine (GEE) to forecast downstream inundation scenarios. Specifically, UAVs were utilized to generate high-resolution Digital Elevation Models (DEMs) of the flood-affected areas, ensuring precise representation of topography in the model. The approach incorporates Cartosat DEM data for catchment modeling, while NASA's Global Precipitation Measurement mission data, integrated with GEE, facilitated accurate estimation of rainfall in ungagged catchment areas. Furthermore, the Hydrological Engineering Center-Hydrological Modeling System was employed for rainfall-runoff simulation and flood hydrograph derivation, followed by application of the HEC River Analysis System (RAS) for hydrodynamic modeling under dam breach conditions. This integrated modeling approach was applied as a case study of Banaskantha district, Gujarat, India. The outcome was the generation of scenario maps based on HEC-RAS results, which include flood extent, water depth, and flow velocity, highlighting downstream areas affected by flooding. Validation of the hydrodynamic dam breach model performance was conducted using actual field measurements and simulated results, employing statistical analysis methods including Support Vector Regression (SVR) and linear regression to determine coefficient of determination ( $R^2$ ), Root-Mean-Square Error, and Mean Absolute Error of observed and simulated data. The coefficient of determination ( $R^2$ ) values for measured and simulated flow (0.91) and water level (0.86) calculated using SVR demonstrate strong correlation between observed and simulated values. This integrated study of hydrodynamic modeling in data-scarce areas aids in accurate estimation of future probable flooding in downstream areas in the event of a dam break, underscoring the potential of advanced surveying and modeling techniques in flood assessment and management. Ultimately, this integration of technologies aims to enhance community resilience and mitigate socioeconomic costs associated with dam breach floods.

**Keywords** Dam breach analysis · Google Earth Engine · Unmanned aerial vehicle · HEC-RAS · HEC-HMS

✉ Indra Prakash  
indra52prakash@gmail.com

Kishanlal Darji  
darjiskishan1@gmail.com

Dhruvesh Patel  
dhruvesh.patel@sot.pdpu.ac.in

Hamad Ahmed Altuwaijri  
haaltuwaijri@ksu.edu.sa

<sup>1</sup> Pandit Deendayal Energy University, Gandhinagar 382426, India

<sup>2</sup> Geological Survey of India, DYDG(R), Gandhinagar 382010, India

<sup>3</sup> Department of Geography, College of Humanities & Social Sciences, King Saud University, Riyadh 11451, Saudi Arabia

## Introduction

The history of water storage through the construction of dams extends back to ancient civilizations, marking the origins of humanity's efforts to harness and manage water resources (Desta and Belayneh 2020). Over time, the importance of dams has grown exponentially, evidenced by the proliferation of hundreds of dams worldwide, each serving a multitude of socioeconomic and environmental purposes (Darji et al. 2024). These structures play crucial roles in providing essential services such as irrigation, drinking water supply, hydropower generation, recreational opportunities, and flood control (Patel et al. 2024). However, despite their numerous benefits, the failure of dams can lead to catastrophic dam breach floods, resulting in extensive loss of life and property damage, particularly in densely populated areas (Derdous et al. 2015; Boussekine and Djemili 2016; Wang et al. 2016; Berghout and Meddi 2016).

The scale of dam infrastructure globally is staggering, with over 800,000 dams distributed across various regions. Among these, approximately 57,000 are classified as major dams, with India ranking third behind the USA and China in terms of large dam ownership (Dhiman and Patra 2019). This widespread distribution underscores the critical need for robust flood management strategies to mitigate the potential consequences of dam failures. While dams have historically played vital roles in water management, instances of dam failures have been relatively sparse in documented history, with notable examples including the Machchu II dam failure in 1979 and the Kaddam dam overtopping disaster in 1958 (Zagonjoli 2007).

In response to the potential hazards posed by dam breaches, the focus has shifted towards improving flood management practices, including developing Emergency Action Plans (EAPs) and implementing effective warning systems (Pandya and Thakor 2013; Patel et al. 2017). Such proactive measures are crucial for minimizing the loss of life and property damage associated with dam breach floods. Dam breach inundation studies play a pivotal role in assessing the safety risks posed by dams, estimating downstream losses, and prioritizing maintenance activities (Gallegos et al. 2009; Pandya and Thakor 2013).

To facilitate accurate prediction of dam breach scenarios and downstream inundation, a range of hydrological and hydrodynamic models have been developed. These models, including the Hydrological Engineering Center's HEC-HMS and HEC-RAS, as well as advanced 2D models like MIKE2 and MIKE11, provide valuable tools for simulating flood events and assessing their potential impacts (Zhang et al. 2019; Darji et al. 2021b, 2022). Recent advancements in modeling techniques have further

enhanced flood prediction capabilities through the integration of remote sensing technologies and high-resolution data sources (Abdessamed and Abderrazak 2019).

In particular, the integration of unmanned aerial vehicles (UAVs), Google Earth Engine (GEE), and satellite imagery has revolutionized flood forecasting accuracy and urban flood management strategies (Yalcin 2019; Darji et al. 2021a; Patel and Pandya 2021). These technologies enable the creation of detailed flood risk maps, evacuation plans, and hazard assessments, empowering communities to better prepare for and respond to flood events (Sahoo and Sreeja 2017; Juliastuti and Setyandito 2017).

This study aims to leverage modern hydrodynamic surveying and modeling approaches, incorporating UAVs, GEE, and satellite imagery, to predict downstream inundation scenarios resulting from dam breach floods. By utilizing HEC-RAS-based 2D hydrodynamic modeling coupled with high-resolution Digital Terrain Models (DTMs) and topographical data obtained from UAVs, the research endeavors to enhance flood prediction accuracy and urban flood management strategies.

## Study area

The study area selected for investigation is the catchment area of Rel River in the Banaskantha district of Gujarat, India. We focus on analyzing the breach of the Jetpura dam (latitude: 24°39'42.73" N, Longitude: 72°17'15.71" E) using the data of the 2017 dam breach flash flood (Fig. 1). The catchment area of the Rel River spans 442 km<sup>2</sup> and is situated between latitudes 24°50' N and 24°75' N, and longitudes 72°00' E and 72°45' E. Notably, the lowest point in the region lies near Dhanera taluka and Dhanera city, close to the mouth of the Rel River.

Characterized as a data-scarce region, the Rel River possesses only one river gauge and rain gauge within its entire catchment area. The river's width measures approximately 280 m at the Road Bridge and 180 m at the Railway Bridge. Notably, the riverbed slope from the upstream of the railway bridge to the downstream of the causeway location is estimated to be about 1 in 500. The upper catchment of the Rel River exhibits a steep topography, contributing to flash flooding downstream. Normally the Rel River catchment is not affected by natural floods except in the year 2015 where a flood was recorded 273 m<sup>3</sup>/s. However in the year 2017 catastrophic flood of 3355 m<sup>3</sup>/s was recorded due to part of the sudden break of the Jetpura dam.

This dam is a masonry cum Earth Dam spans a total length of 1240 m (comprising 1155.50 m of an earthen dam and 84.50 m of a masonry dam) and a height of 10 m. The dam's catchment area measures 99.71 km<sup>2</sup>, with a gross storage capacity of 25.02 lakh M<sup>3</sup>. Notably, heavy rainfall

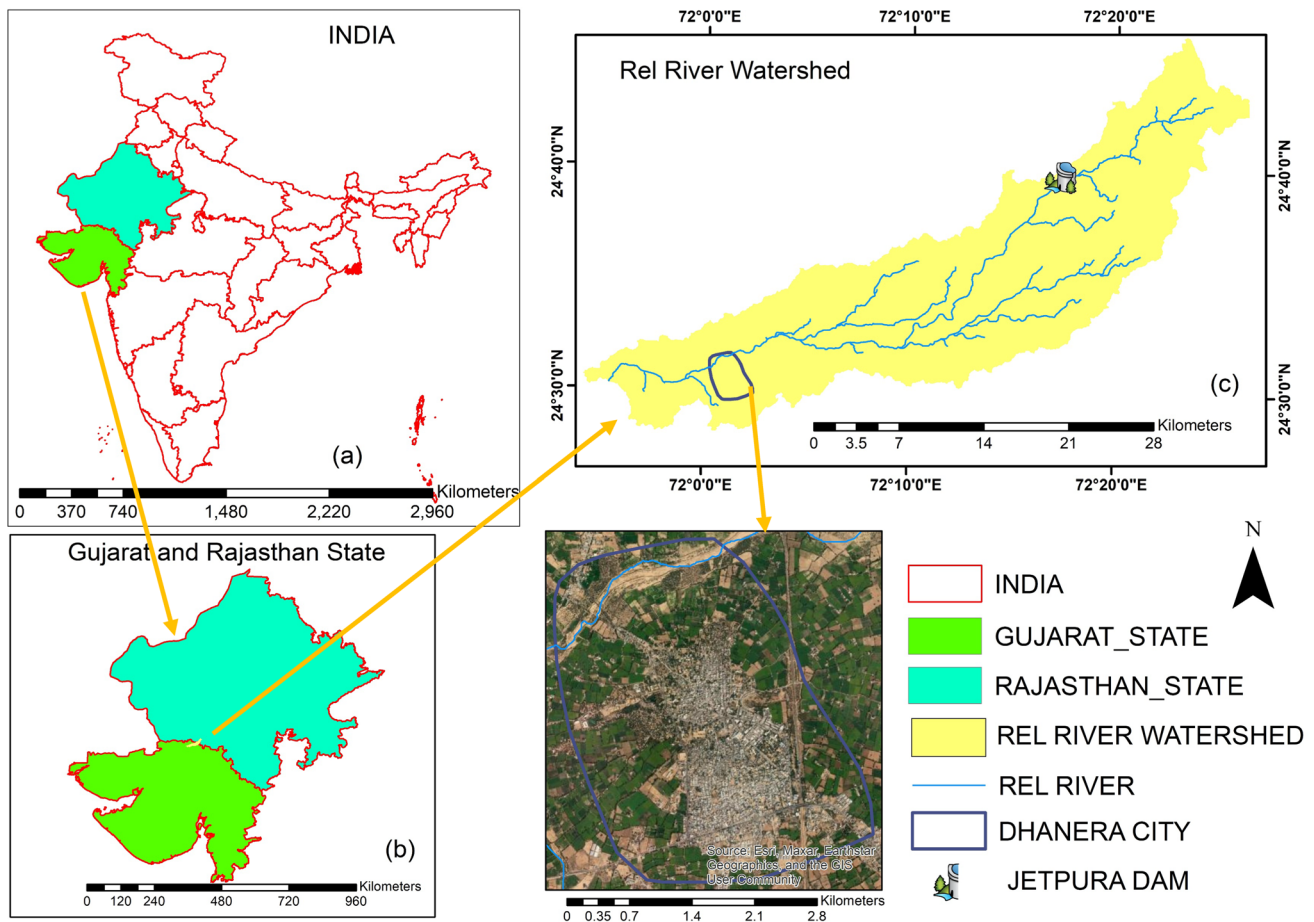


Fig. 1 Study area representing the location of Rel River watershed, Jetpura dam, and Dhanera city

exceeding 50 mm/hour on July 24, 2017, led to the breach of the 210 m earthen part of Jetpura dam, triggering a flash flood downstream.

### Overview of the 2017 Jetpura dam breach disaster

The 2017 Jetpura dam breach, triggered by heavy rainfall on July 24th, unleashed a devastating flood across the Rel River catchment, inundating numerous villages and the city of Dhanera with an average water depth ranging from 2.5 to 3 m (Fig. 2a). The catastrophic event resulted in significant human and economic losses, as reported by the Times of India ([https://en.wikipedia.org/wiki/2017\\_Gujarat\\_flood](https://en.wikipedia.org/wiki/2017_Gujarat_flood)), with approximately 72 fatalities, the loss of 81,609 cattle (Fig. 2b, c), and property damage estimated at 2.72 billion USD across Banaskantha, Patan, and Kachchh districts. Dhanera bore the brunt of the flood, experiencing the highest level of inundation compared to other cities in the Banaskantha district.

The flood's impact extended beyond loss of life and property. Over 370 roads, including vital national and state highways, were submerged, disrupting vehicular traffic. The damage to transportation infrastructure was substantial, with estimated losses of 12.91 million USD for national highways and 33.57 million USD for state highways. The disruption also affected rail travel, with 11 out of 20 Mumbai-Delhi train services canceled due to track damage near Palanpur. Additionally, 915 GSRTC bus trips were canceled in northern districts.

The scale of the disaster necessitated a large-scale evacuation effort, with more than 113,000 individuals relocated to safety. The financial toll of the disaster was significant, with losses estimated at 2.32 billion USD for agricultural production and land, 953.17 million USD for damaged highways and roads, and additional demands for the restoration of irrigation facilities and public infrastructure, totaling over 2.19 billion USD. Despite these efforts, comprehensive data on flood extent, damage assessment, and affected areas remained elusive, underscoring the urgent need for advanced modeling techniques to better understand flood dynamics and aid in future mitigation planning.



**Fig. 2** **a** Dhanera city market under the flood up to 2–3 m, **b** cattle (cow) died in flood 2017 (The Times of India), **c** NDRF team rescued the flood susceptible people from the low-lying areas. (Photographs

retrieved from <https://timesofindia.indiatimes.com/city/ahmedabad/flood-fury-hits-gujarat-25000-people-evacuated/articleshow/59744404.cms>)

In response to the Jetpura disaster, this study proposes the integration of hydrodynamic modeling with cutting-edge remote sensing technologies, including satellite imagery, unmanned aerial vehicles (UAVs), and Google Earth Engine (GEE), to assess dam breach floods and predict downstream inundation scenarios. By leveraging these tools, we aim to enhance flood risk assessment, improve disaster response strategies, and minimize the impact of similar catastrophic events in India and beyond.

## Methodology

The study commenced with the selection of the Rel River watershed, followed by an exhaustive compilation of meteorological and satellite data to gain comprehensive insights into the prevailing environmental conditions. In this area large-scale topographic maps were not available, therefore a high-resolution Digital Elevation Model (DEM) was generated using unmanned aerial vehicles (UAVs). Subsequently, HEC-HMS hydrological modeling techniques were employed to generate runoff flow hydrographs of the upstream catchment area of the dam. These data were used as input in the 2D HEC-RAS hydrodynamic model for dam breach analysis. Different flood scenario maps were generated to visualize and analyze probable downstream flood areas (Fig. 3). Finally, to evaluate the performance of the model, statistical measures were employed, including Support Vector Regression (SVR) and linear regression (LR) (Table 1).

## Data collection and generation

### River gauge data collection

River gauging is vital for understanding river behavior, particularly during flood events. In this study, river

discharge and water level data were collected from a gauge station located at the NH168A bridge in Dhanera city. These data, obtained from the Dhanera Taluka Panchayat and the Dhanera Road and Building Department, offered insights into the flow dynamics of the Rel River during the 2017 flood event. For instance, on July 24, 2017, at 10:00 am, the maximum discharge recorded was 3335 m<sup>3</sup>/s, with a corresponding river level of RL 135 m (Fig. 4).

### DEM-CARTOSAT

Digital Elevation Models (DEMs) are crucial for hydrological modeling, providing information on terrain elevation. The CARTOSAT-1 DEM, developed by the Indian Space Research Organization (ISRO), was utilized in this study. With a spatial resolution of 10 m, CARTOSAT-1 data covered the Rel River catchment area (Fig. 5). These data were essential for delineating flood-prone areas and understanding topographic features influencing flood propagation. Despite limitations such as cloud cover, CARTOSAT-1 DEM offered high accuracy compared to other DEM sources.

### Soil map creation

Soil characteristics play a significant role in hydrological processes, affecting water infiltration rates and runoff patterns. A soil map at a 1:50000 scale was generated using data from various sources, including the Ahmedabad agricultural department, the National Resources Information System (NRIS), and the National Bureau of Soil Survey and Land Use Planning. This map classified soils into five different textures, providing insights into soil–water interactions within the study area (Fig. 6).



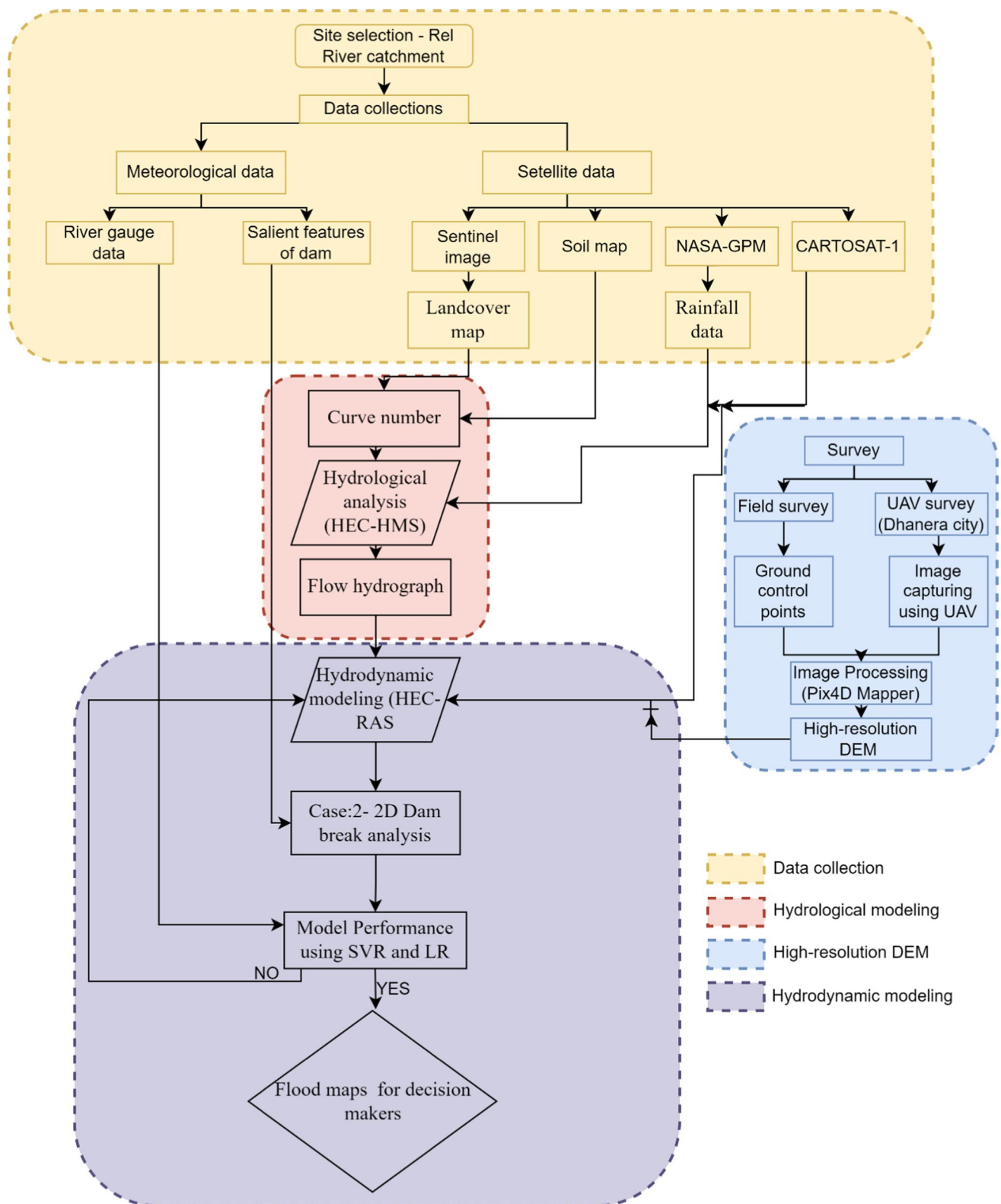


**Fig. 3** Methodology flow chart, phase-1: data collection, phase-2: hydrological modeling, phase-3: generation of high-resolution DEM, phase-4: hydrodynamic modeling

**Table 1** Data collection with their sources

Sr. no	Particulars	Source
1	Rainfall data	State Water Data Center and NASA GPM
2	River gauge data	State Water Data Center
3	Digital elevation model	Indian Space Research Organisation
4	Land use data	Sentinal-2 data
5	Soil data	National Resources Information System (NRIS)

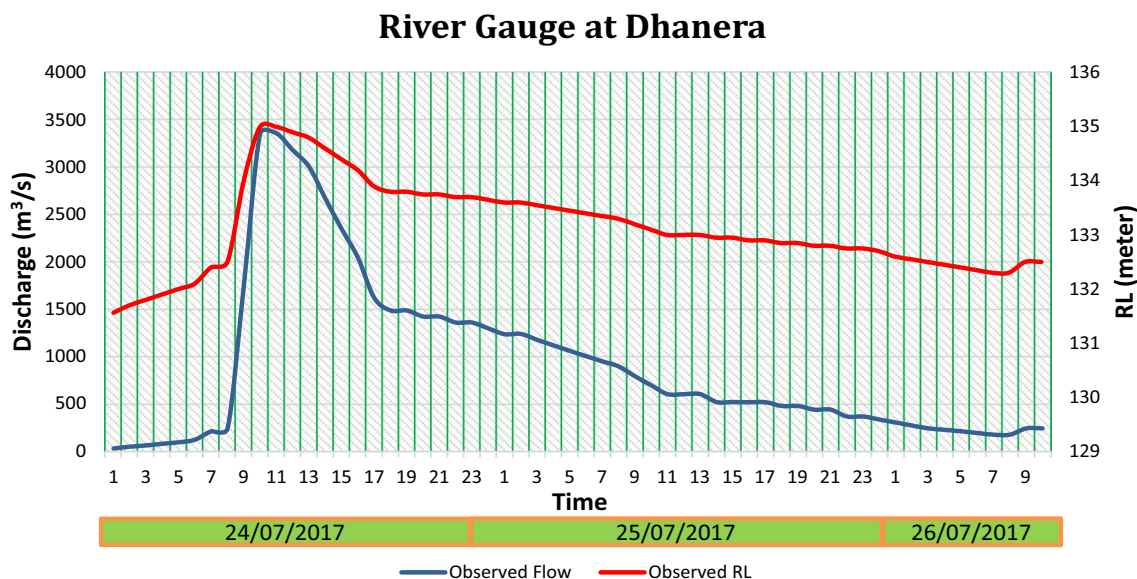


**Fig. 4** River gauge data showing discharge and water levels at location of Dhanera bridge (July 24, 2017, to July 26, 2017)

**Land use and land cover maps creation**

Land cover types influence surface runoff and infiltration rates, impacting flood dynamics. Sentinel-2 satellite data, with its multi-spectral capabilities, were employed to generate a land cover map of the research region (Fig. 7). Supervised classification techniques were applied using the maximum likelihood algorithm in the Sentinel Application Platform (SNAP). Additionally, toposheets and Google Earth imagery were utilized to refine the classification accuracy. The resulting land use and land cover map provided crucial information for hydrological modeling and flood risk assessment.

**Rainfall data generation from Google Earth Engine**

Precipitation data, crucial for understanding the dynamics of water movement, are often measured in millimeters or inches. Within our research area, two rain gauge stations, Bapla and Dhanera, provide valuable rainfall observations. The Bapla station, located near the Gujarat-Rajasthan border on the upstream side of the catchment, contrasts with the Dhanera station, which is positioned downstream at

the Prathmik Arogya Kendra in Dhanera. Unfortunately, observed rainfall data for the 2017 event are not available for the Bapla gauge. However, daily rainfall records for this event were obtained from the Dhanera gauge, sourced from the Gujarat State Water Data Center (GSWDC). Daily rainfall data, though informative, may not be adequate for detailed modeling of rainfall-runoff dynamics, especially individual events. To supplement these records and enable more robust analysis, we utilized near-real-time rainfall monitoring techniques. Leveraging NASA's Integrated Multi-satellite Retrievals for GPM (IMERG) half-hourly data, derived from a combination of ground-based and air-borne instruments, we achieved higher temporal resolution in rainfall measurements. This advanced dataset supports the validation of satellite-based retrieval algorithms, ensuring the accuracy of the precipitation inputs.

Additionally, the Global Satellite Mapping of Precipitation (GSMaP) offers estimates of global hourly rain rates at a resolution of 0.1×0.1 degrees. Drawing from this resource, we accessed NASA-GPMaP hourly rainfall data for the Rel River catchment area using Google Earth Engine (GEE). This dataset was instrumental in simulating runoff model and assessing the precision of the modeling outcomes. By

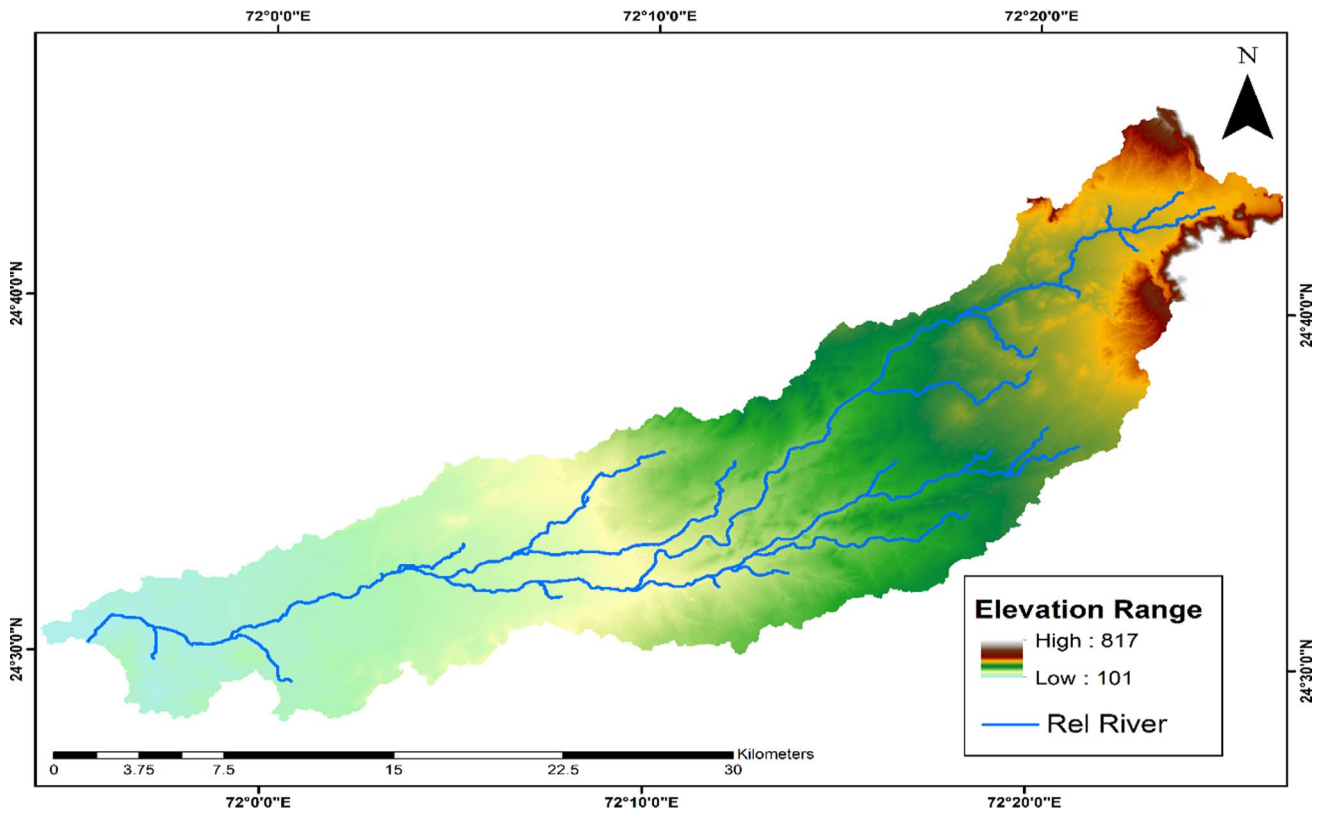


Fig. 5 CARTOSAT DEM of Rel River catchment

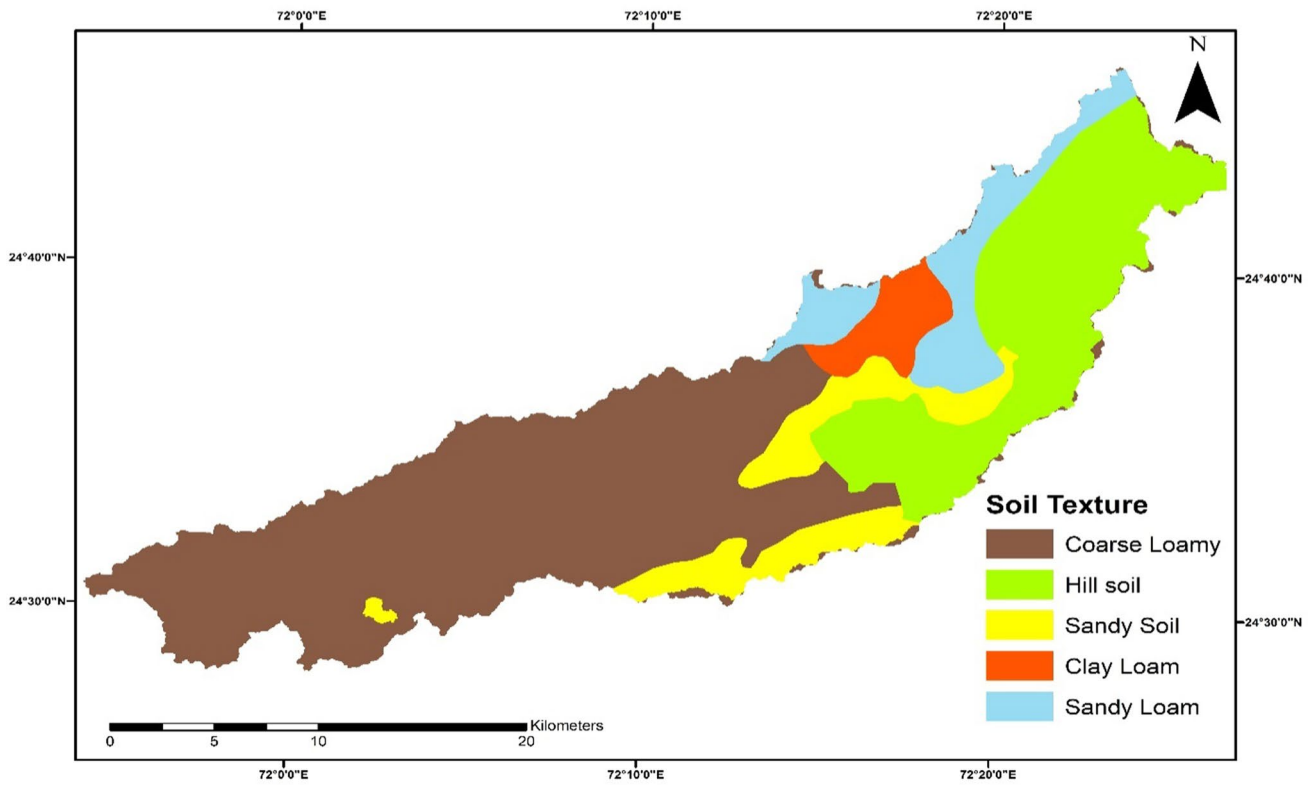
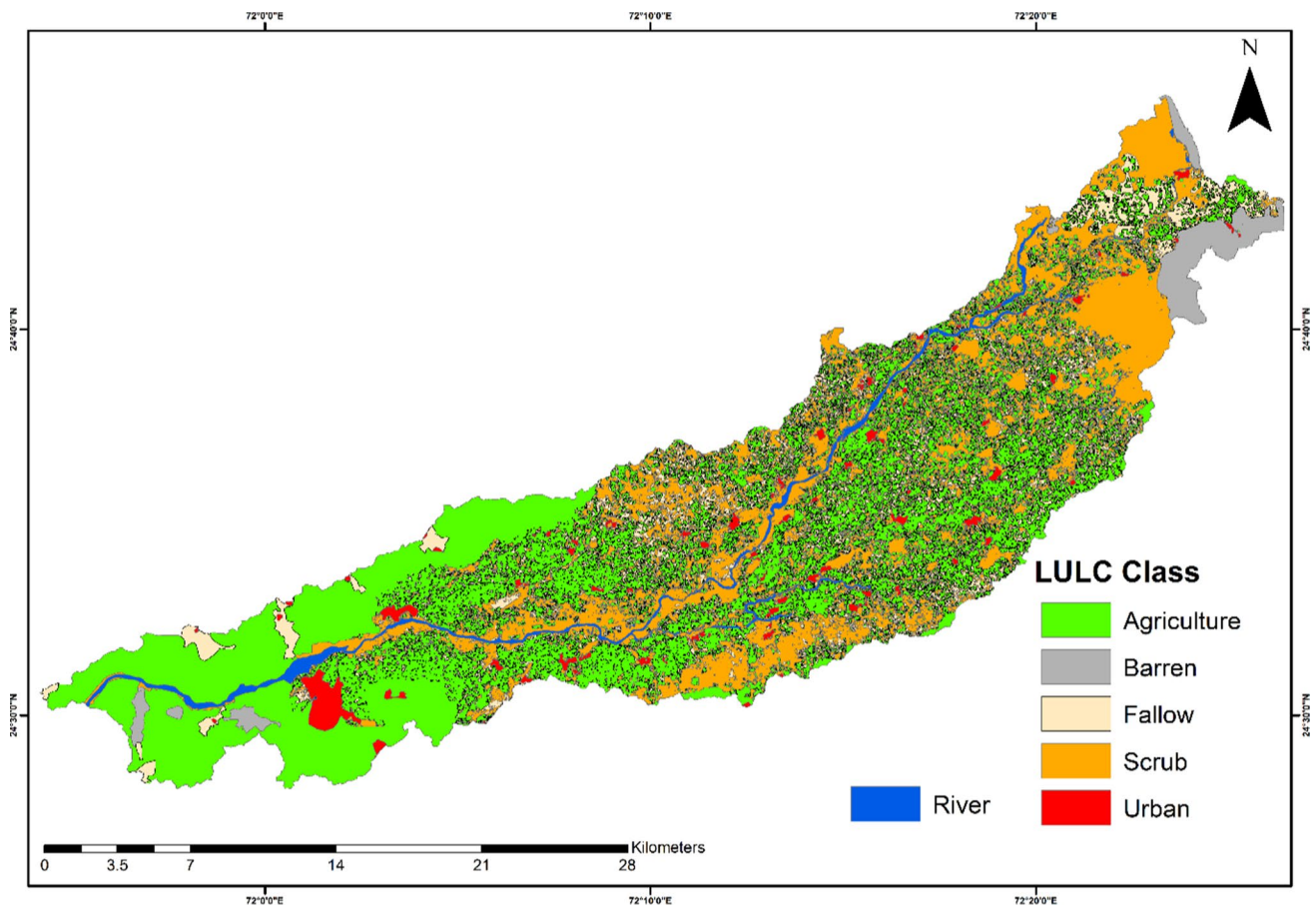


Fig. 6 Soil classification map of Rel River catchment



**Fig. 7** Land use classification map of Rel River catchment

integrating these high-resolution precipitation datasets, we enhance the accuracy and reliability of the hydrodynamic modeling efforts, ultimately improving understanding of dam breach floods and downstream inundation scenarios.

#### High-resolution DEM generated from UAV survey

To acquire detailed topographic information essential for accurate hydrodynamic modeling, a high-resolution survey was conducted using a DJI Phantom4 Pro RTK unmanned aerial vehicle (UAV). Operating with automatic flight capabilities at an altitude of 130 m above ground level, the UAV covered the target area with an 80% overlap to ensure comprehensive image capture.

Equipped with a digital, 4 K-resolution FC300X camera mounted on its lower section, the UAV provided high-quality imagery for mapping purposes. With a 20-megapixel sensor, 2.8 mm focal width, and RGB band functionality, the camera delivered detailed visual data suitable for precise terrain modeling. Operating in both manual and automatic modes, it ensured flexibility and efficiency in image acquisition.

A total of 9222 aerial photographs were acquired during the UAV survey, covering an area of 10 km<sup>2</sup> encompassing Dhanera city. To enhance the accuracy of the resulting DEM, field surveys were conducted to mark Ground Control Points (GCPs) across the study area. These reference points facilitated precise georeferencing and alignment of the aerial imagery.

Subsequent data processing was conducted using PIX4D-mapper software, involving three key stages: initial processing, point cloud and mesh generation, and final processing. In the initial phase, key point extraction algorithms identified distinctive features within the aerial images, forming the basis for subsequent analysis. Through the utilization of point cloud and mesh tools, the dataset underwent densification, resulting in the generation of additional tie points aimed at augmenting spatial resolution and detail.

In the final processing stage, a high-resolution DEM of the area was generated, capturing intricate terrain features with exceptional accuracy. The resulting DEM served as a vital component in hydrodynamic modeling endeavors, providing detailed elevation data crucial for simulating flood scenarios and assessing downstream inundation risks.



By integrating the UAV-derived high-resolution DEM with existing CARTOSAT data, a comprehensive elevation model of the Rel River basin was produced. This combined dataset forms the foundation for hydrodynamic modeling efforts, enabling precise analysis and prediction of dam breach floods and associated inundation scenarios with confidence and accuracy.

## Modeling

The hydrological and hydrodynamic dam breach model was developed utilizing the data collected from various sources, including rainfall records, topographic surveys, and other relevant data sources. The model was then calibrated and validated with historical flood data from the 2017 event.

### Hydrological modeling

Advancements in hydrological studies across various disciplines, including computer science, geographic information systems (GIS), and remote sensing, have been bolstered by the support of universities, research centers, and organizations invested in the hydrological field. These collective efforts have yielded significant progress, leading to the creation of hydrological computer programs and models. Furthermore, these advancements have facilitated the accessibility of enhanced and current databases encompassing basin characteristics, watercourses, and the factors that exert influence within these systems (Abdelkarim et al. 2019).

For hydrological simulation in this study, the HEC-HMS software package, a freeware tool developed by the US Army Corps of Engineers, was employed. This modeling approach relies on a lumped conceptual model, utilizing physical sub-basin characteristics and hydrological data as inputs.

HEC-HMS comprises three modules: basin, meteorological, and control models, providing a comprehensive framework for hydrological analysis. During the simulation of runoff in the Rel River catchment for the 2017 flash flood event, the catchment was divided into two sub-basins to facilitate accurate modeling (Fig. 8). "River140" represents a river segment automatically generated by HEC-HMS modeling software.

To estimate precipitation loss and evaluate direct runoff, the Soil Conservation Service Curve Number (SCS-CN) method was utilized. This method is referred to as Type II, and it is the most widely used (Abdelkarim et al. 2019). This method, as documented by (Elfeki et al. 2016; Vojtek and Vojteková 2016; Darji et al. 2022), and (Zhang et al. 2020), calculates precipitation loss based on the Curve Number (CN) value. The CN value, ranging from 0 to 100, reflects the runoff potential of the area: Lower values indicate lower runoff potential, while higher values indicate increased runoff potential.

The selection of this method was informed by its effectiveness in similar hydrological studies. By employing the SCS-CN method, accurate modeling of runoff dynamics in the Rel River catchment was achieved, contributing to the comprehensive assessment of flood risk and mitigation strategies.

$$S = \frac{25400}{CN} - 254 \quad (1)$$

$$I_a = \lambda S \quad (2)$$

According to Subramanya (2013),  $\lambda$  is 0.3 for Indian environmental conditions.

The direct runoff ( $Q$ ) and net rainfall for the catchment can be determined using initial abstraction ( $I_a$ ), average precipitation ( $P$ ), and potential maximum retention ( $S$ ) values in the following equation

$$Q = \frac{(P - I_a)^2}{P - I_a + S} \quad (3)$$

Runoff occurs only when rainfall exceeds  $I_a$ , therefore  $Q=0$  when precipitation is lower or equal to initial abstraction ( $P \leq \lambda S$ ). The rainfall loss was calculated using Eqs. 1, 2, and 3 of the SCS-CN approach. Weighted curve numbers for each subbasin were calculated using a land cover and soil map (Cronshey et al. 1985; Subramanya 2013). The base flow was overlooked because it was small in comparison with the severe precipitation that occurred during flash flood episodes. Other physical properties estimated with the HEC GeoHMS included stream length, slope, elevation, centroidal location, and longest flow path. The control specification specifies the start and end times of the simulation, as well as the time step (Liu et al. 2021). The flood hydrographs for both basins were used as input data to perform hydrodynamic modeling.

### Hydrodynamic dam breach modelling

The HEC-RAS 6.1, a widely used hydrodynamic model developed by the US Army Corps of Engineers, can perform one-dimensional (1D), two-dimensional (2D), and coupled 1D-2D hydraulic calculations of water surface profiles in various natural and constructed channel network configurations (Lastra et al. 2008; Bout and Jetten 2018; Jha and Afreen 2020; Naeem et al. 2021; Darji and Patel 2024). For the 2017 dam breach flood event (July 24, 2017), a two-dimensional 2D dam breach unsteady flow simulation of HEC-RAS based on 2D diffusive wave equations was validated for the Gujarat Rel River watershed. Under dam breach unsteady flow, the upstream border is a discharge hydrograph generated from hydrological modeling and

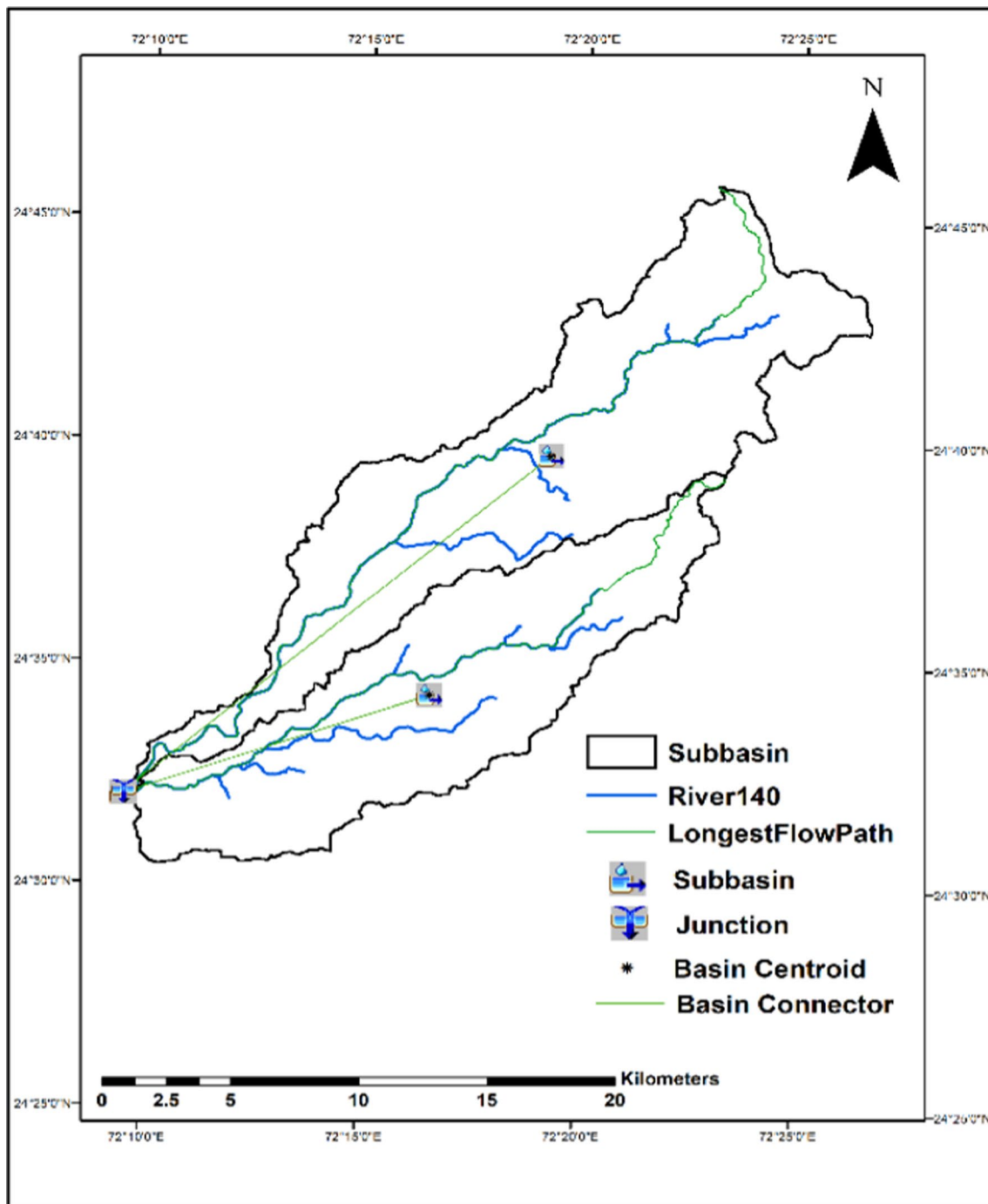


**Fig. 8** Basin model created by HEC-GeoHMS

storage of the reservoir, whereas the downstream boundary is normal depth. The overtopping dam breach criteria include a variety of factors important for determining the probable consequences of a breach event. These criteria include the type of dam and its geometry (height, width, slope, and elevation), which all influence breach development and subsequent water flow. Additionally, parameters like the initial breach size, growth rate, and formation time

are critical for understanding the evolution of the breach during flooding, location of the breach along the dam structure, inflow conditions from reservoir levels, and upstream flow rates. This overtopping dam breach parameters were examined using news, field surveys, and Google Photos for simulation. The model calculates discharges and stages for all interior sites. Additionally, Manning's roughness ( $n$ ) values for the model domain were determined using LULC

data. HEC-RAS version 6.1 solves unsteady flow simulations using diffusion wave equations (Quiroga et al. 2016).

$$\frac{\partial \xi}{\partial t} + \frac{\partial p}{\partial x} + \frac{\partial q}{\partial x} = 0 \tag{4}$$

$$\begin{aligned} \frac{\partial p}{\partial t} + \frac{\partial}{\partial x} \left( \frac{p^2}{h} \right) + \frac{\partial}{\partial y} \left( \frac{pq}{h} \right) = & - \frac{n^2 pg \sqrt{p^2 + q^2}}{h^2} \\ & - gh \frac{\partial \xi}{\partial x} + pf + \frac{\partial}{\partial x} (h\tau_{xx}) + \frac{\partial}{\partial y} (h\tau_{xy}) \end{aligned} \tag{5}$$

$$\begin{aligned} \frac{\partial q}{\partial t} + \frac{\partial}{\partial x} \left( \frac{q^2}{h} \right) + \frac{\partial}{\partial y} \left( \frac{pq}{h} \right) = & - \frac{n^2 qg \sqrt{p^2 + q^2}}{h^2} \\ & - gh \frac{\partial \xi}{\partial y} + qf + \frac{\partial}{\partial y} (h\tau_{yy}) + \frac{\partial}{\partial x} (h\tau_{xy}) \end{aligned} \tag{6}$$

where  $h$  is water depth in meters,  $p$  and  $q$  are the specific flow in the  $x$  and  $y$  direction ( $m^2 s^{-1}$ ),  $n$  is the surface elevation in meters,  $g$  is the acceleration due to gravity,  $n$  is the Manning resistance,  $q$  is the water density ( $kg m^{-3}$ ),  $s_{xx}$ ,  $s_{yy}$ , and  $s_{xy}$  are the components of the effective shear stress, and  $f$  is the Coriolis ( $s^{-1}$ ).

The HEC-RAS model generates elevation of water level, depth of water, velocity of water, rating curves, hydraulic parameters, and flood visualizations. This generated map will help to prepare the emergency action plans to decide flood conditions.

### Model performance

To determine the accuracy of the HEC-RAS simulation, a Support Vector Regression (SVR) and linear regression (LR) technique was used to compare observed and simulated data at the Dhanera bridge gauge station.

#### Linear regression

LR is a statistical method used to model the relationship between a dependent variable  $Y$  and independent variables  $x_1, x_2, x_3, \dots, x_n$ . The model assumes a linear relationship between the variables and seeks the best-fitting linear equation that predicts the dependent variable's value using the independent variables. The equation representing LR is as follows:

$$Y = mx + c \tag{7}$$

where  $Y$  is a dependent variable,  $x$  is an independent variable,  $m$  is the slope of the regression line, and  $c$  is the  $y$ -intercept. During model training, the approach reduces the residual sum of squares (RSS) or mean squared error (MSE) between observed and predicted values by using optimization techniques such as ordinary least squares (OLS). LR models are frequently evaluated using measures like

Root-Mean-Squared Error (RMSE),  $R$ -squared, and Mean Absolute Error (MAE).

#### Support Vector Regression

Support vector machines (SVMs) are intelligent computational models used for classification and regression analysis. Regression analysis identifies correlations between the dependent variable  $Y$  and independent variable  $X$ . A kernel function is used to map the relationship and explain how estimated  $Y$  differs from computed values (Fig. 9) (Darji et al. 2023). The SVR model is formulated as a convex optimization problem, aiming to minimize the regularization term  $\frac{1}{2} \|W\|^2$  subject to the constraints  $|Y_i - \langle W, X_i \rangle + B| \leq \epsilon$  for all  $i$ . Introducing slack variables ( $\xi_i$ ) and ( $\xi_i^*$ ) To handle infeasible constraints, the optimization problem becomes:

$$\left[ \min \frac{1}{2} \|W\|^2 \right] + \left[ C \sum_{i=1}^n (\xi_i + \xi_i^*) \right] \tag{8}$$

subject to the constraints:

$$\begin{aligned} Y_i - \langle W, X_i \rangle + B & \leq \epsilon + \xi_i \text{ for all } i \\ \langle W, X_i \rangle + B - Y_i & \leq \epsilon + \xi_i^* \text{ for all } i \\ \xi_i, \xi_i^* & \geq 0 \end{aligned}$$

where  $W$  is hyperplane orientation,  $B$  is intercepted,  $C$  is the penalty parameter controlling the trade-off between maximizing the margin and minimizing the classification error, ( $\xi_i$ ) and ( $\xi_i^*$ ) is slack variables,  $\epsilon$  is the epsilon-insensitive loss function parameter, and  $n$  is the numbers of samples.

To determine the best model, SVR models with radial basis function (RBF) kernels are developed and trained with various regularization parameter  $C$  values. The performance of each model is evaluated using the Root-Mean-Squared Error

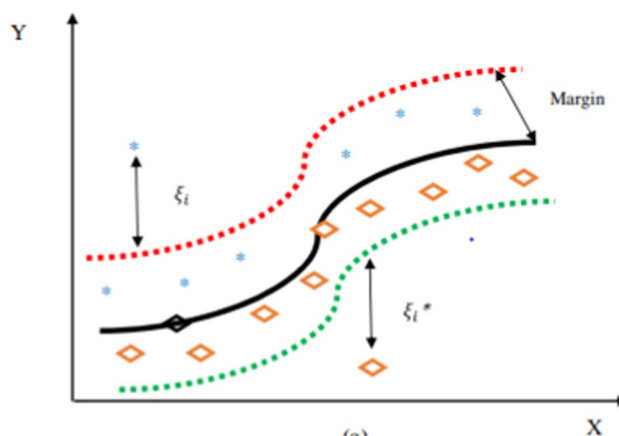


Fig. 9 Regression analysis using Support Vector Regression (adapted from Darji et al. 2023)

(RMSE). The RMSE values for various  $C$  values are plotted to show how the value of  $C$  impacts the model's performance. In addition, the final SVR model with the best-performing  $C$  value is used to estimate water levels, and the model's accuracy is assessed using the RMSE, Mean Absolute Error (MAE), and  $R$ -squared. Finally, a scatter plot is constructed to compare the observed and anticipated water levels, along with an ideal fit line, which provides information about the model's accuracy.

**Mean Absolute Error (MAE)** Mean Absolute Error (MAE) has been used to analyze the performance of the observed and simulated data. The difference between the simulated value and the observed value is calculated by:

$$\text{MAE} = \frac{1}{n} \sum_{i=1}^n |\odot_i - \odot| \quad (9)$$

Here,  $\odot_i$  shows the observed value;  $\odot$  shows the simulated value.

**Root-Mean-Square error (RMSE)** Root-Mean-Square Error (RMSE) represents the standard deviation of the residuals. RMSE is commonly used in hydrology, forecasting, and regression analysis to verify experimental results.

$$\text{RMSE} = \frac{1}{n} \sqrt{\sum_{i=1}^n (\odot_i - \odot)^2} \quad (10)$$

where  $i$  is the variable,  $n$  represents data points,  $\odot_i$  represents observed value, and  $\odot$  represents simulated value.

**$R$ -squared ( $R^2$ )**  $R$ -squared provides insight into the proportion of variance in the observed data explained by the model. It is calculated using the formula:

$$R = 1 - \frac{\sum_{i=1}^n (\odot_i - \odot)^2}{\sum_{i=1}^n (\odot_i - \underline{\odot})^2}$$

where  $\odot_i$  represents the observed value,  $\odot$  represents the simulated value, and  $\underline{\odot}$  represents the mean of the observed values.

By comparing observed and simulated flow values, the study aims to provide useful insights into the dependability and accuracy of the HEC-RAS model in modeling flood events and predicting flow dynamics in the Rel River.

## Results

In this section, the outcomes of simulating the 2017 dam breach flood event within the Rel River catchment are presented. Various parameters including flood depth, water

surface level, velocity, arrival time, duration, and flood inundation were meticulously simulated. The innovative approach offers distinct advantages over conventional hydrodynamic modeling techniques. Firstly, it facilitates the acquisition of high-resolution data crucial for developing precise hydrodynamic models. Secondly, it harnesses the capabilities of Unmanned Aerial Vehicles (UAVs) to gather supplementary data, thereby enhancing model accuracy. Additionally, it harnesses the computational power of Google Earth Engine (GEE) to process hourly rainfall data, further refining result accuracy.

The model operates within a 2D environmental framework, incorporating flood hydrographs upstream and normal depths downstream. The flood hydrograph is meticulously crafted through hydrological modeling, employing the Soil Conservation Service Curve Number (SCS-CN) approach within the HEC-HMS model. Validation through simulating the dam breach scenario corroborates the 2017 flood event.

The findings demonstrate the effectiveness of the proposed approach in forecasting downstream inundation scenarios. Model accuracy was rigorously assessed utilizing SVR such as the coefficient of determination ( $R^2$ ). The  $R^2$  values obtained for predicted water depths stand at 0.86, indicative of a strong correlation between predicted and observed values.

### Hourly rainfall generated from GEE

Hourly rainfall for 2017 events on July 23, 24, and 25 was derived from NASA-GPM satellite data using the Google Earth Engine. Figure 10 shows that the greatest rainfall value of 57.727 mm occurred on July 24, 2017, at 05:00 a.m. These hourly rainfall data were used to simulate runoff, yielding an accurate hourly flood hydrograph for hydrodynamic modeling.

### UAV-based high-resolution digital elevation model (DEM)

A total of 9222 photographs were captured using a DJI Phantom4 Pro RTK through automatic flight operations, maintaining an altitude of 130 m above ground level. These images were captured with an 80% overlap, covering a sprawling 10 km<sup>2</sup> area. To ensure comprehensive coverage and accuracy, the entire area was divided into four zones for detailed picture analysis within Pix4D mapper software. This meticulous process generated a comprehensive dataset comprising a point cloud, a Digital Surface Model (DSM), and a Digital Terrain Model (DTM).

Upon completion of the processing phase, the four individual DTMs were seamlessly merged to create a unified, high-resolution DEM of the Dhanera city region, as depicted in Fig. 11. The DSM and DEM derived from the UAV



### Rainfall (mm)

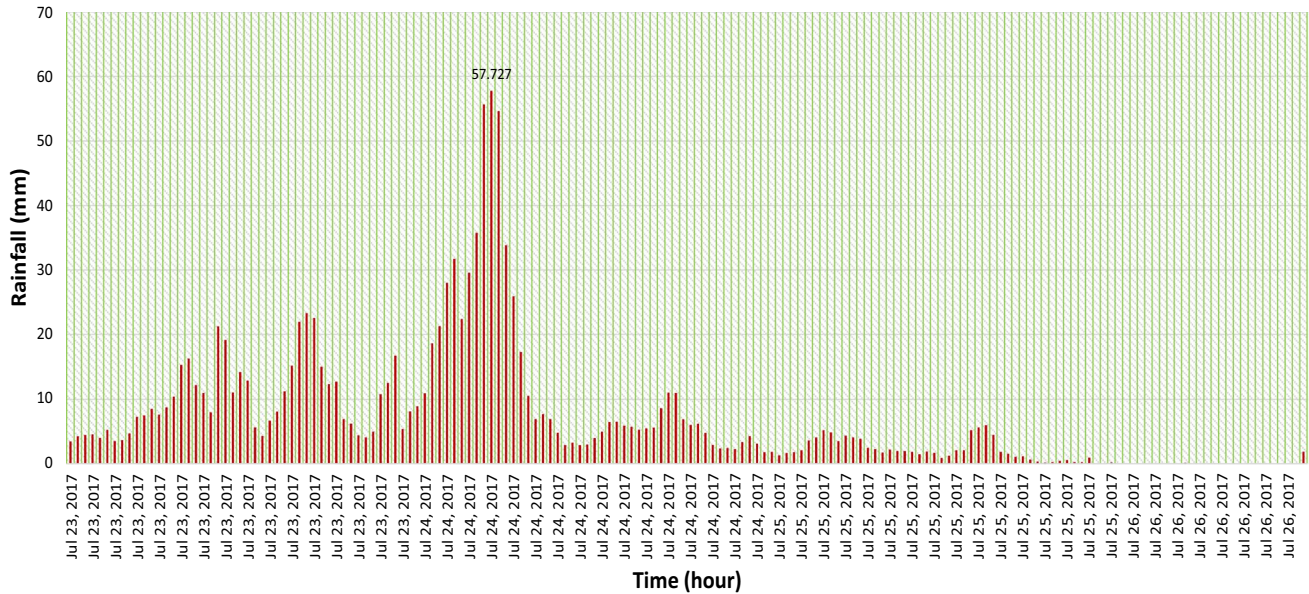


**Fig. 10** Hourly rainfall derived from NASA-GPM satellite data with the help of Google Earth Engine period from July 23, 2017, to July 26, 2017

imagery exhibit impressive resolutions of  $3.6 \times 3.6$  centimeters and  $10 \times 10$  cm, respectively.

After the creation of the high-resolution DEM, adjustments were made to the datum, transitioning from ellipsoid height to geoid height. This meticulous correction process ensures alignment and compatibility with existing geospatial data standards. The resulting combined DEM, augmented by the integration of data from the CARTOSAT DEM, served as a pivotal tool in enhancing hydrodynamic simulation accuracy and precision.

### Flow hydrograph generated from hydrological modeling

Flood hydrographs provide a visual representation of how a drainage basin reacts to precipitation events. In this study, flood hydrographs were meticulously crafted utilizing the Soil Conservation Service Curve Number (SCS-CN) approach within the HEC-HMS model. This approach enabled the modeling of the response of both the main Rel River and one of its major tributaries to the rainfall patterns observed during the 2017 event (Fig. 12).

The HEC-HMS model was employed to generate hydrographs for two distinct basins: W370 representing the main river basin, and W360 representing a significant tributary. These basins were characterized by unique Curve Number (CN) values, reflecting their land cover, soil characteristics, and impervious surfaces. Specifically, the weighted curve numbers calculated for W370 and W360 were 71.67 and

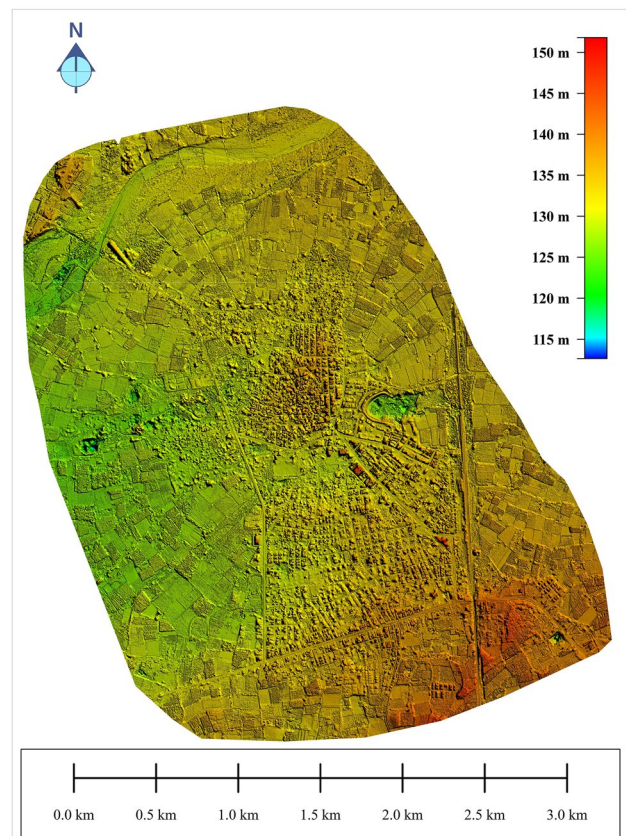


**Fig. 11** 10 cm \* 10 cm high-resolution DEM of Dhanera city generated from UAV survey technique

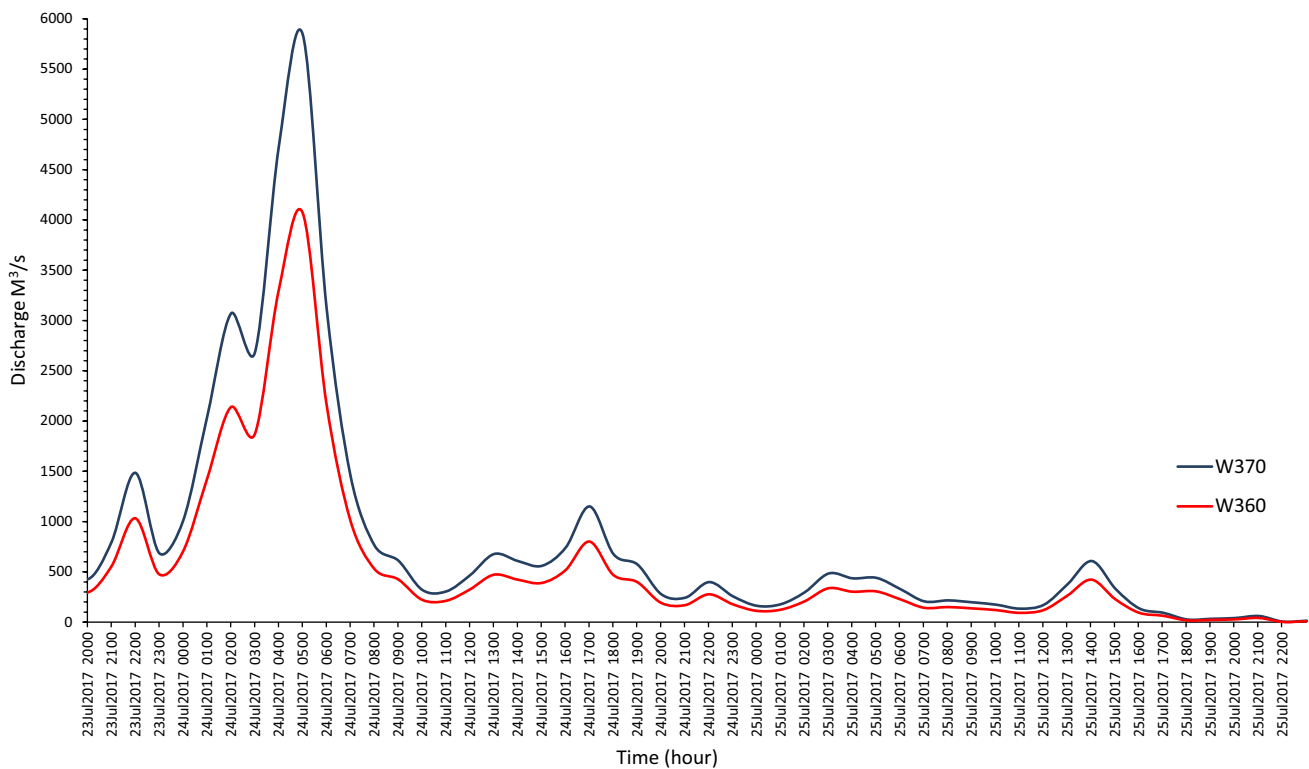


**Fig. 12** Flood hydrograph of watershed W370 and W360 starting from 23rd July 20:00 to 25th July 22:00 of 2017 event

73.01, respectively, indicating a moderately high runoff potential within these catchments.

The resulting flood hydrographs depicted peak flow rates of  $5838 \text{ m}^3/\text{s}$  for basin W370 and  $4069 \text{ m}^3/\text{s}$  for basin W360. These values underscore the significant flow dynamics within these hydrological systems during the 2017 event. Importantly, these flood hydrographs served as critical upstream boundary conditions for subsequent hydrodynamic simulations, providing essential input parameters for modeling downstream inundation scenarios with greater accuracy and precision.

### Hydrodynamic assessment of dam breach flooding

In this study, we conduct a comprehensive assessment of the 2017 flood event utilizing 2D hydrodynamic modeling of dam breach unsteady flow. The simulation spans from July 23, 2017, at 20:00 to July 24, 2017, at 23:00, capturing critical temporal and spatial dynamics of the flooding event. Key parameters such as water depth, velocity, surface elevation, and inundation area are extracted from the simulation results, providing valuable insights into the extent and severity of the flooding.

Furthermore, we focus on the breach analysis of the Jetpura dam, employing a 2D framework within the HEC-RAS 6.1 simulation model. The dam's storage capacity is

reported to be 25.02 lakh  $\text{m}^3$ , with a high flood level reaching 252.50 m RL. Through rigorous investigation, including consultation with local residents and verification via satellite imagery, it was confirmed that the dam breach occurred over a span of 210 m within a 10 min on July 24, 2017, around 07:00 a.m.

These validated parameters are subsequently utilized for the simulation work. By integrating data obtained from various sources, including Google Earth imagery, we generate detailed maps depicting water surface elevation, depth, velocity, and inundation areas using ArcMap. This comprehensive approach allows us to accurately assess the impact of the dam breach, providing critical information for disaster mitigation and management efforts.

**Water Depth** The analysis reveals significant variations in water depth across the affected areas. Notably, within the dam storage vicinity, depths peak at 12 m (Fig. 13), while certain stretches of the river exhibit depths ranging from 7 to 8 m. Extensive inundation, covering approximately  $24 \text{ km}^2$ , is characterized by depths between 1 and 1.5 m. Out of the total area of  $126 \text{ km}^2$ ,  $21.6 \text{ km}^2$  and  $15.4 \text{ km}^2$  experience inundation depths of 1.5–2 m and 2 to 2.5 m, respectively. This detailed depth information serves as a cornerstone for developing emergency evacuation strategies, providing crucial insights for decision-makers.

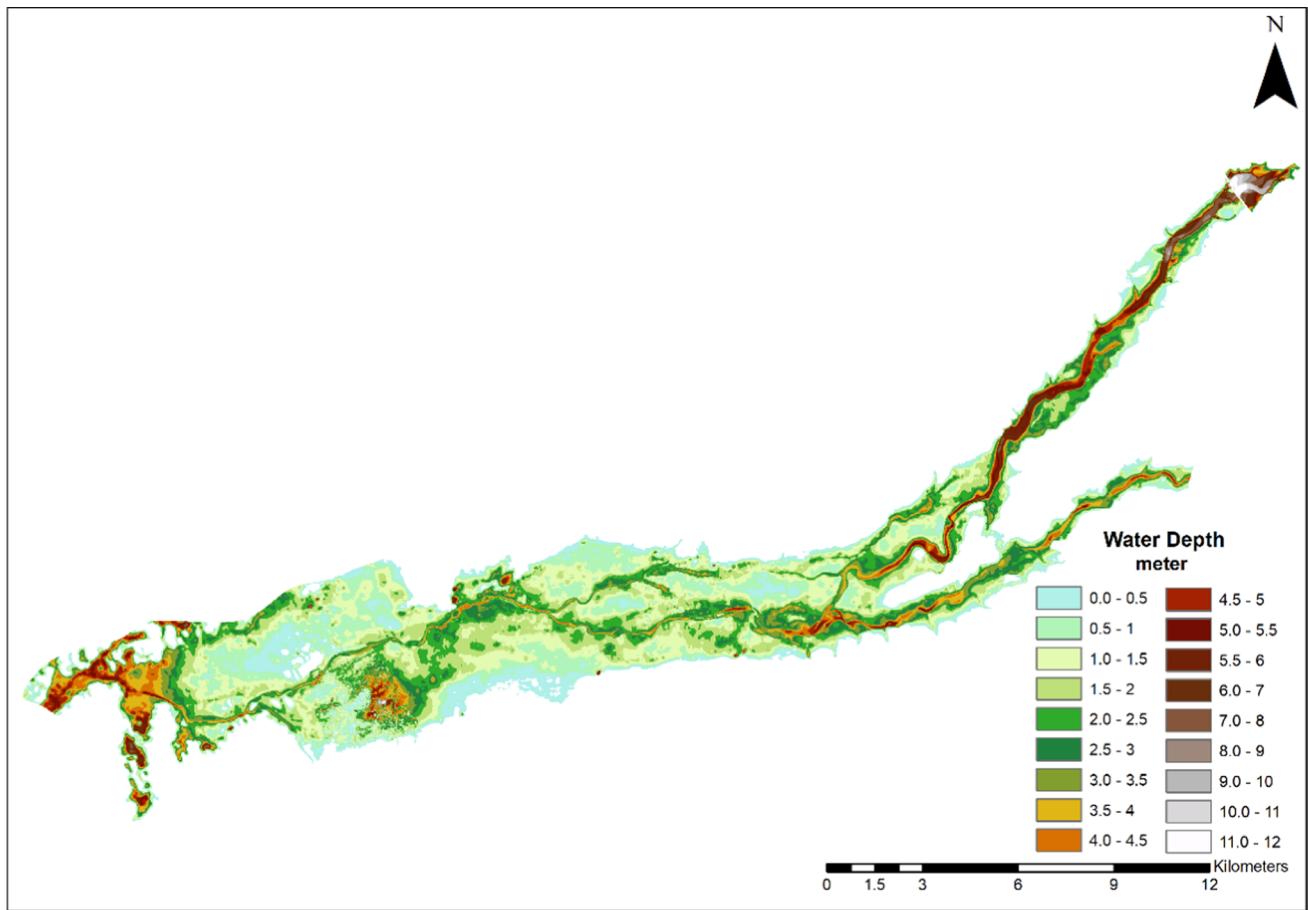


**Fig. 13** Maximum water depth map derived from 2D hydrodynamic dam breach modeling

**Water Inundation** The inundation map derived from the dam break simulation delineates a total inundated area of 126 km<sup>2</sup> (Fig. 14). The onset of the deluge is marked by inundation at Mewada village at 00:00 h on July 24, 2017, followed by subsequent inundation events. Rampura Mota village succumbs to flooding by 01:00 h on the same day, while Nagala, Rajoda, Malotra, and Sera villages witness inundation by 4:00 p.m. On July 24, 2017, Dhanera was completely submerged by 8:00 p.m., with Sankad, Jorapura, Dhakha, and Rampura villages experiencing inundation by 11 a.m. This chronological inundation progression is invaluable for decision-makers in formulating evacuation plans and issuing timely notifications to mitigate potential fatalities.

**Water Surface Elevation** Fig. 15 illustrates water surface elevations relative to the main sea level. This mapping provides crucial data for understanding the spatial distribution of floodwaters and assessing potential risks to infrastructure and communities.

**Velocity of Flow** Analysis of flow velocities, as depicted in Fig. 16, highlights significant variations in flow dynamics. Upstream regions exhibit higher velocities, reaching

5–6.5 m/s, while downstream velocities range from 1.5 to 2.5 m/s. The average water velocity ranges from 1 to 2 m per second, providing essential information for assessing the intensity and speed of floodwaters across different sections of the river.

### Model performance evaluation

To assess the effectiveness of the model, we conducted a rigorous LR and SVR analysis comparing observed and simulated flow and water level data obtained from the Dhanera bridge. The results of this analysis provide valuable insights into the model's accuracy and reliability in predicting flood dynamics. Mean Absolute Error (MAE), Root-Mean-Square Error (RMSE), and *R*-Square (*R*<sup>2</sup>) were used to identify the performance of the HEC-RAS model.

### Comparison between observed and simulated water level

To compare observed and simulated water levels, the LR and SVR techniques were used. A comparison of LR and



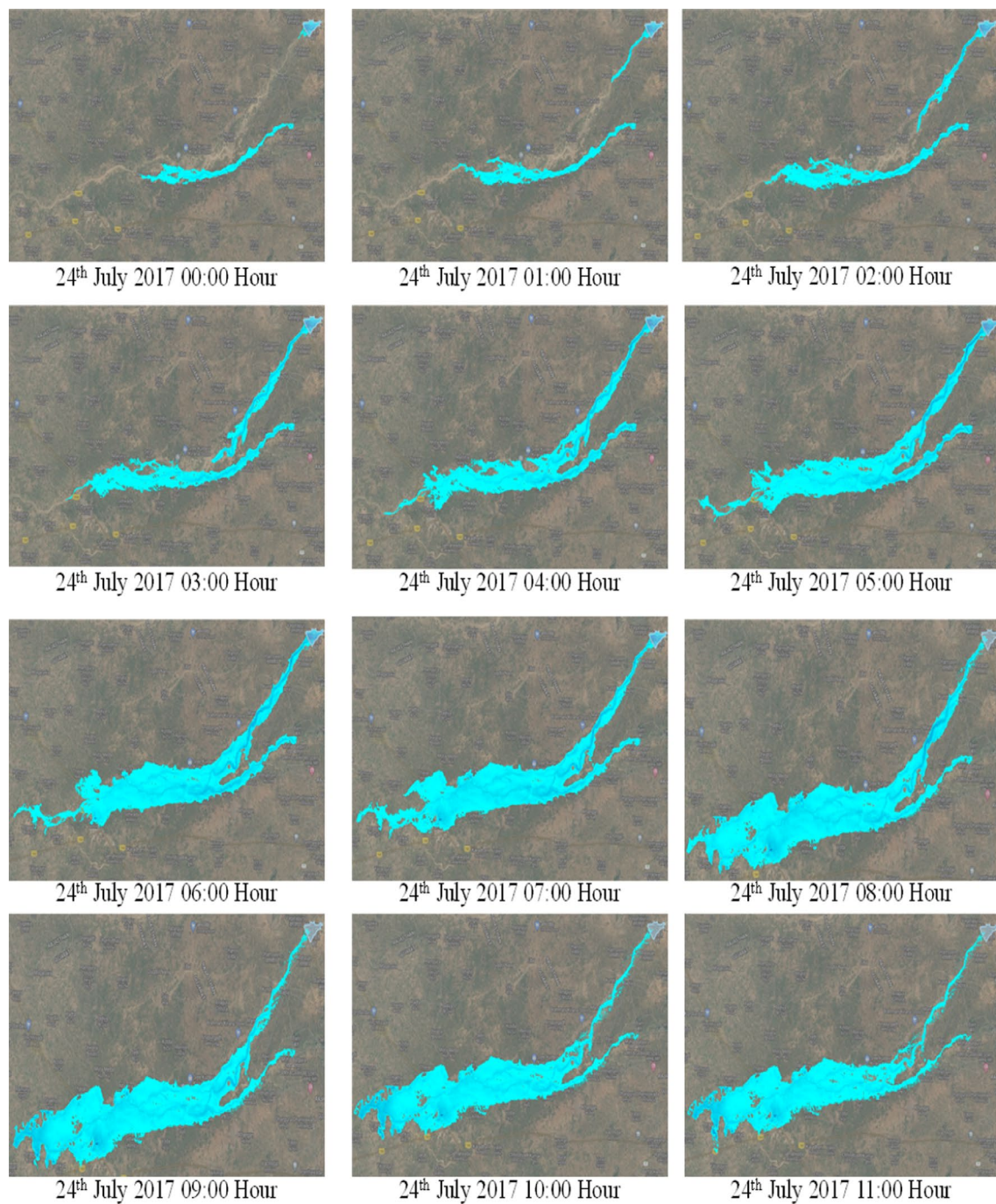


**Fig. 14** Water inundation scenario starting from 24th July 00:00 to 11:00 of 2017 event derived from 2D hydrodynamic dam breach modeling

SVR for observed and simulated water levels indicates significant differences in model performance. In the initial analysis, the SVR model's Root-Mean-Square Error (RMSE) was minimized at a C value of 1000 (Fig. 17), suggesting a significant agreement between observed and simulated water levels. LR provides a Root-Mean-Square error (RMSE) of 2.78 m, suggesting a modest amount of prediction inaccuracy; however, SVR drastically reduces the RMSE to 0.28 m,

displaying greatly increased accuracy in forecasting water levels.

Similarly, the *R*-square score for LR is 0.82, indicating a decent fit of the model to the data, whereas SVR has a higher *R*-square of 0.86, indicating greater explanatory power and capacity to capture the variance in observed water levels. Furthermore, the Mean Absolute Error (MAE) for LR is calculated to be 2.75 m, but SVR obtains a significantly



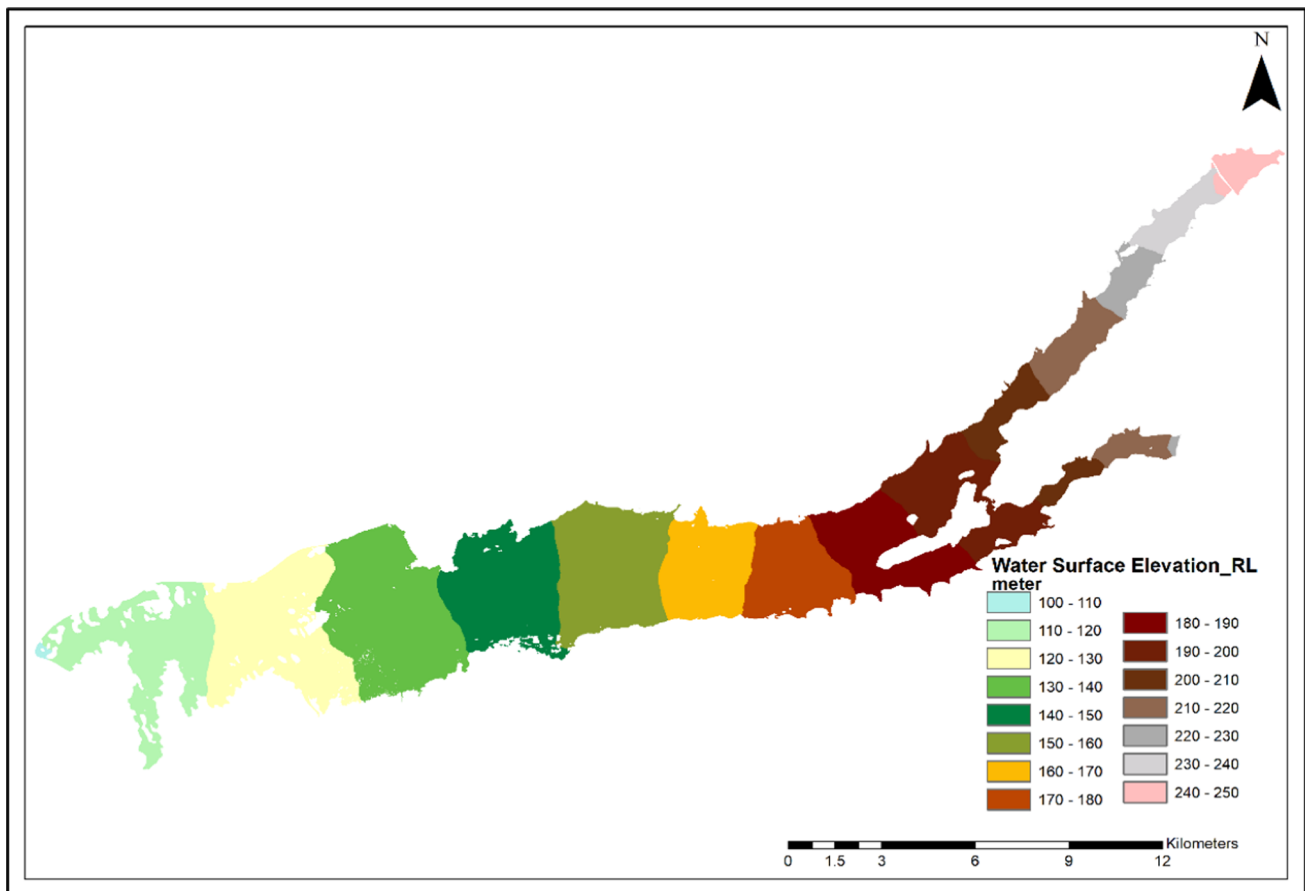


**Fig. 15** 2D hydrodynamic dam breach modeling simulated water surface elevation map

lower MAE of 0.2 m, demonstrating its greater accuracy in forecasting water levels with less average absolute discrepancies between observed and simulated values. A scatter chart based on LR and SVR of observed and simulated water levels graphically demonstrates the model's performance (Fig. 18a and b). Overall, SVR is better than LR by providing a good correlation between observed and simulated water levels at the Dhanera bridge gauge station (Fig. 19).

#### Comparison between observed and simulated water flow

The comparison of actual and simulated flow using LR and SVR provides light on the effectiveness of both methods for modeling water flow at the Dhanera bridge gauge station. The SVR model's Root-Mean-Square Error (RMSE) was minimized at a  $C$  value of 100 (Fig. 20), suggesting a significant agreement between observed and simulated water flow.

The linear regression approach produced a Root-Mean-Square Error (RMSE) of 652.71, but SVR performed better with an RMSE of 254.09. This shows that SVR

provided a more accurate description of the observed flow than linear regression. Linear regression achieved an  $R$ -squared score of 0.87, whereas SVR had a slightly higher  $R$ -squared of 0.91. The coefficient of determination ( $R$ -squared) reflects the proportion of the variation in the dependent variable that is predictable from the independent variable. This suggests that SVR captured a greater share of the variability in the observed flow data, showing a higher goodness of fit than linear regression. Furthermore, while calculating the Mean Absolute Error (MAE), which evaluates the average absolute difference between observed and predicted values, linear regression had an MAE of 494.35, but SVR had a significantly lower MAE of 180.75. This means that SVR produced flow closer to the observed values on average, demonstrating its higher accuracy at the Dhanera bridge gauge station (Fig. 21a and b). A scatter chart based on linear regression and SVR of observed and simulated water levels graphically demonstrates the model's performance (Fig. 22).

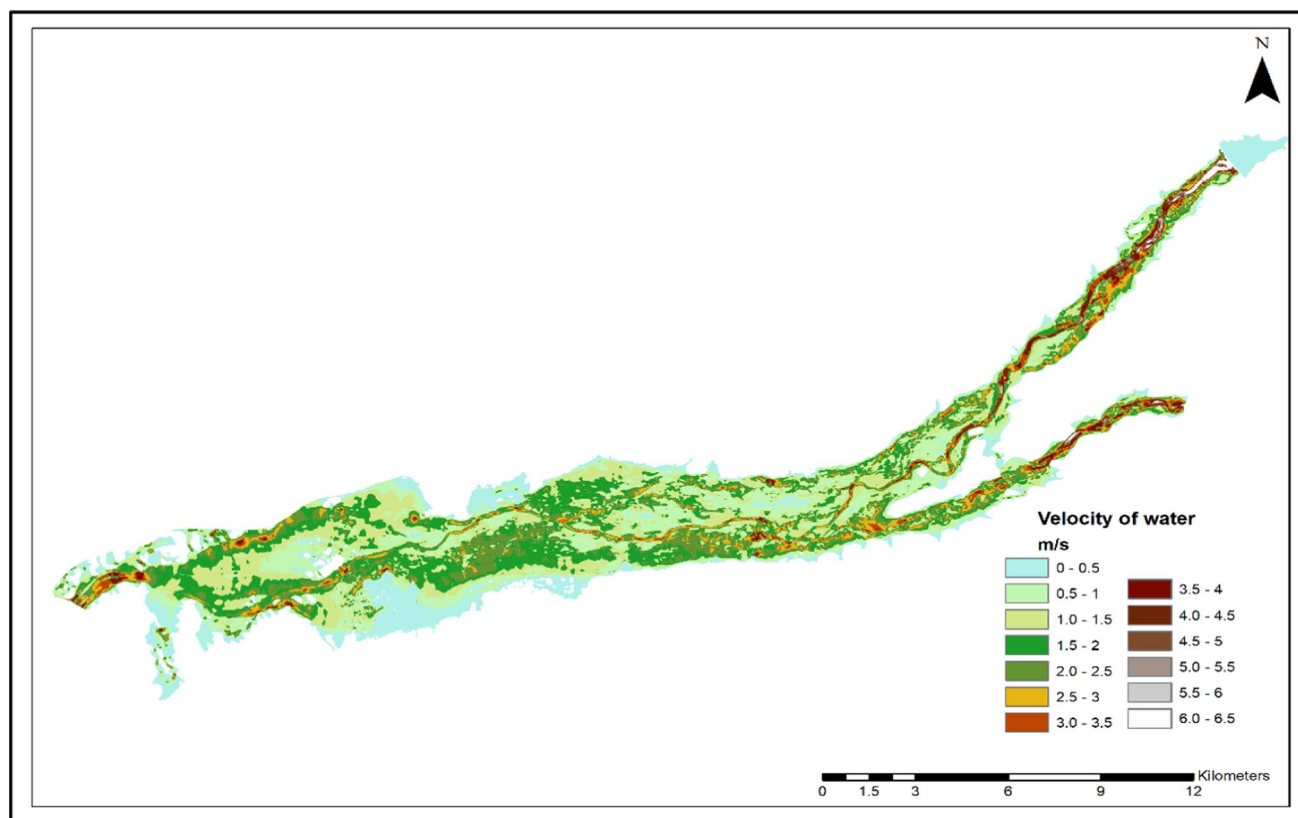


**Fig. 16** Velocity map derived from 2D hydrodynamic dam breach modeling

## Discussion

Flood control, assessment, and management are complex endeavors, exacerbated by the multifaceted nature of flood events influenced by various climatic and geographic factors. The integration of advanced technologies and modeling techniques has revolutionized flood risk measurement, enhancing effectiveness and efficiency in flood management (Flood Risk Discussion Paper 2019). For instance, (Matgen et al. 2007) utilized Synthetic Aperture Radar (SAR)-derived flood coverage maps and precise topographic data to generate detailed water depth maps for the River Alzette in Luxembourg, showcasing the potential of remote sensing in flood modeling.

Similarly, (Borah et al. 2018) employed SAR data to delineate inundation zones in Kaziranga National Park, demonstrating the applicability of remote sensing in identifying vulnerable areas prone to flooding. Moreover, (Pathan et al. 2022a) effectively utilized 2D HEC-RAS-based hydrodynamic modeling to simulate various flood scenarios, providing valuable insights for flood risk management and mitigation planning.

The significance of data resolution, particularly the mesh grid size, cannot be overstated in flood simulation models

(Pathan et al. 2022b). A finer mesh grid ensures model stability and accuracy, enhancing the reliability of flood predictions. Additionally, (Trambadia et al. 2022) leveraged open-source data, including SRTM and ALOS DEMs, for 1D hydrodynamic modeling, emphasizing the importance of utilizing diverse data sources for comprehensive flood analysis.

However, the computational demands associated with 2D hydrodynamic models pose challenges, limiting their application to scenarios requiring real-time forecasts or extensive simulations (do Lago et al. 2023). To address this, emerging technologies such as deep learning and conditional generative adversarial networks (cGAN) offer promising avenues for predicting floods in areas with variable border conditions, leveraging large datasets for accurate modeling (do Lago et al. 2023).

Furthermore, continuous simulation approaches, as advocated by (Acuña and Pizarro 2023), provide flood managers with comprehensive time series data, augmenting traditional flood statistics with detailed temporal insights. This holistic approach enables a deeper understanding of flood dynamics, facilitating proactive measures for flood mitigation and response. In this study comparison between observed and simulated data was made using SVR and LR for simulating

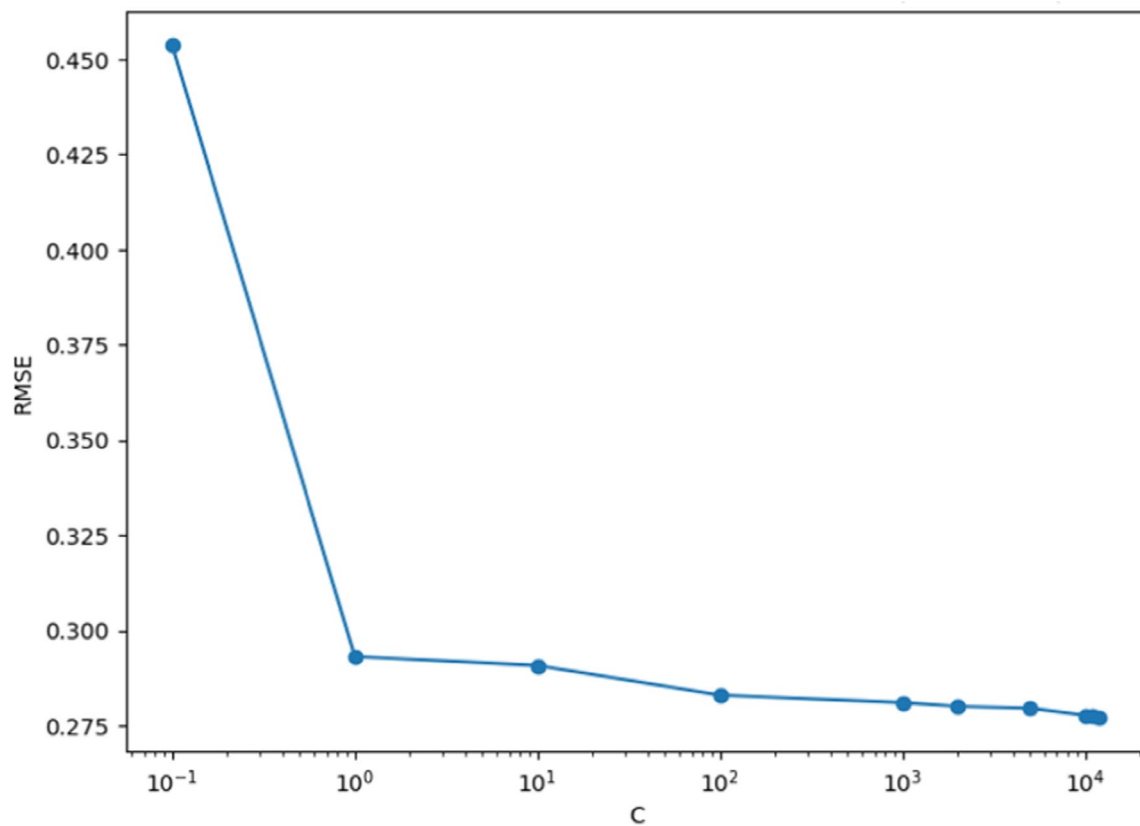


Fig. 17 RMSE for different  $C$  values in SVR for water levels

water level and water flow dynamics; the results highlight the superior performance of SVR in terms of accuracy metrics such as RMSE, R-squared, and MAE. The lower RMSE and MAE values, coupled with the higher R-squared value, indicate that SVR provides more accurate and reliable results of flow dynamics compared to linear regression. This underscores the importance of leveraging advanced modeling techniques like SVR, particularly in data-scarce regions, to improve flood management practices.

Recent advancements in machine learning and data assimilation techniques have further elevated the efficacy of flood risk assessment. Techniques such as Support Vector Regression (SVR) and Artificial Neural Networks (ANNs) have shown significant promise in predicting flood events with high accuracy (Rezaeianzadeh et al. 2014; Pradhan et al. 2020). SVR, for instance, excels in handling nonlinear relationships in hydrological data, providing robust predictions of water levels and flow dynamics (Khan and Coulibaly 2006). On the other hand, the integration of ANNs with hydrological models has enabled more nuanced simulations, capturing the complexity of flood processes more effectively (Mosavi et al. 2018). Additionally, ensemble modeling approaches that combine multiple machine learning algorithms have emerged as powerful tools, offering enhanced

predictive performance and uncertainty quantification (Darji et al. 2023). These methodologies are particularly beneficial in regions with limited data availability, where traditional models may struggle. Moreover, the synergy between remote sensing technologies and machine learning frameworks has opened new avenues for real-time flood monitoring and early warning systems, thereby significantly improving the resilience of flood-prone communities (Singh et al. 2023). Such interdisciplinary approaches underscore the critical role of continuous innovation and collaboration in advancing flood management practices and mitigating the adverse impacts of flooding.

In light of these advancements, the proposed approach in this study, integrating high-resolution satellite imagery, UAVs, and Google Earth Engine, represents a significant stride forward in flood modeling (Flood Risk Discussion Paper 2019). By leveraging cutting-edge technologies and innovative modeling techniques, it holds promise for enhancing flood risk assessment, management, and mitigation strategies. However, ongoing research and collaboration are essential to address existing challenges and fully harness the potential of these advancements in safeguarding communities against the devastating impacts of flooding.

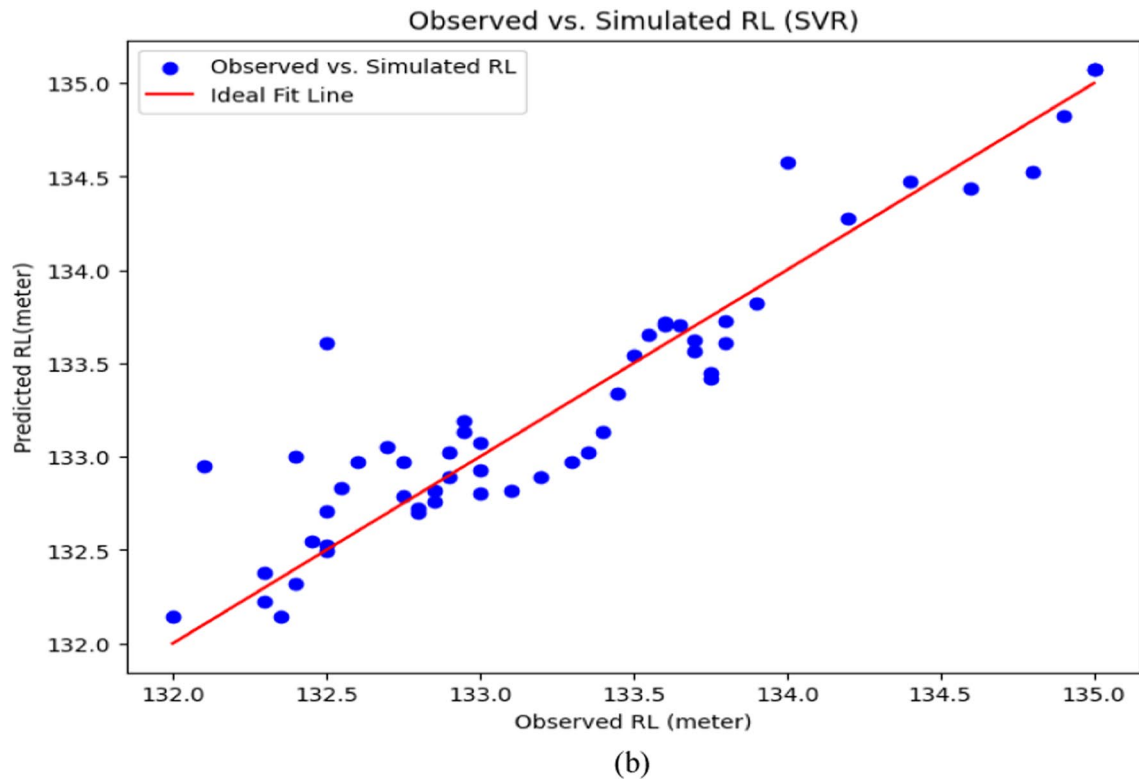
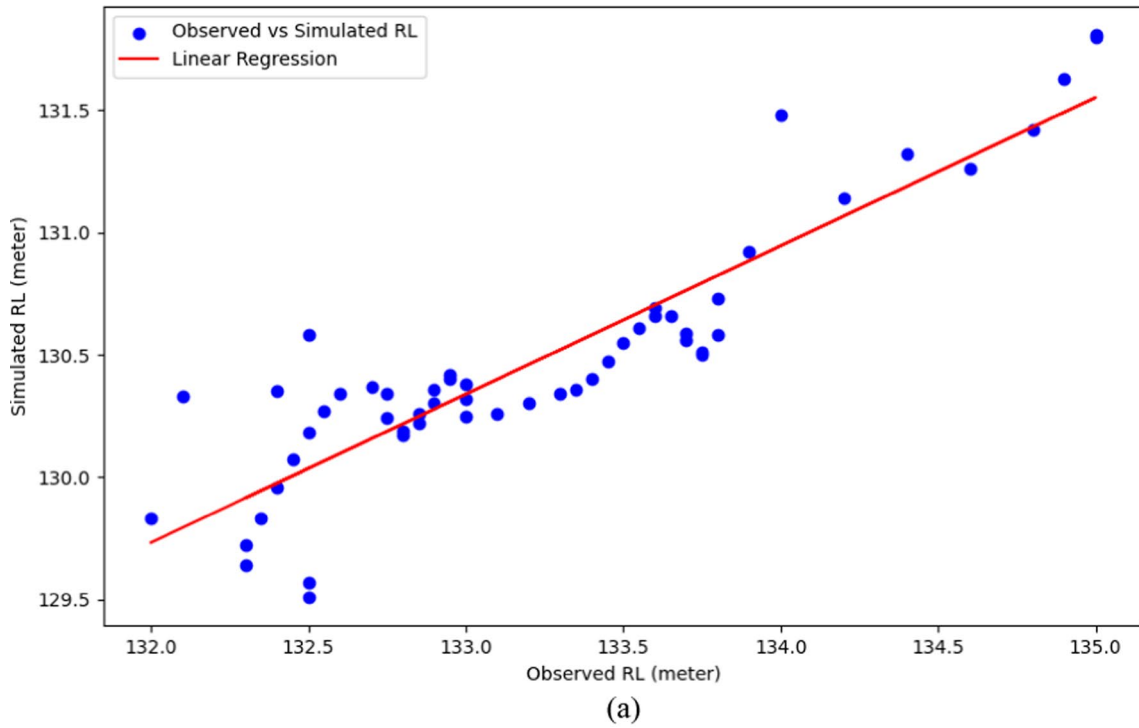


**Fig. 18** Comparison of observed and simulated water level at Dhanera bridge gauge station using **a** linear regression, **b** SVR



**Fig. 19** Model performance of observed and simulated water level using linear regression and SVR

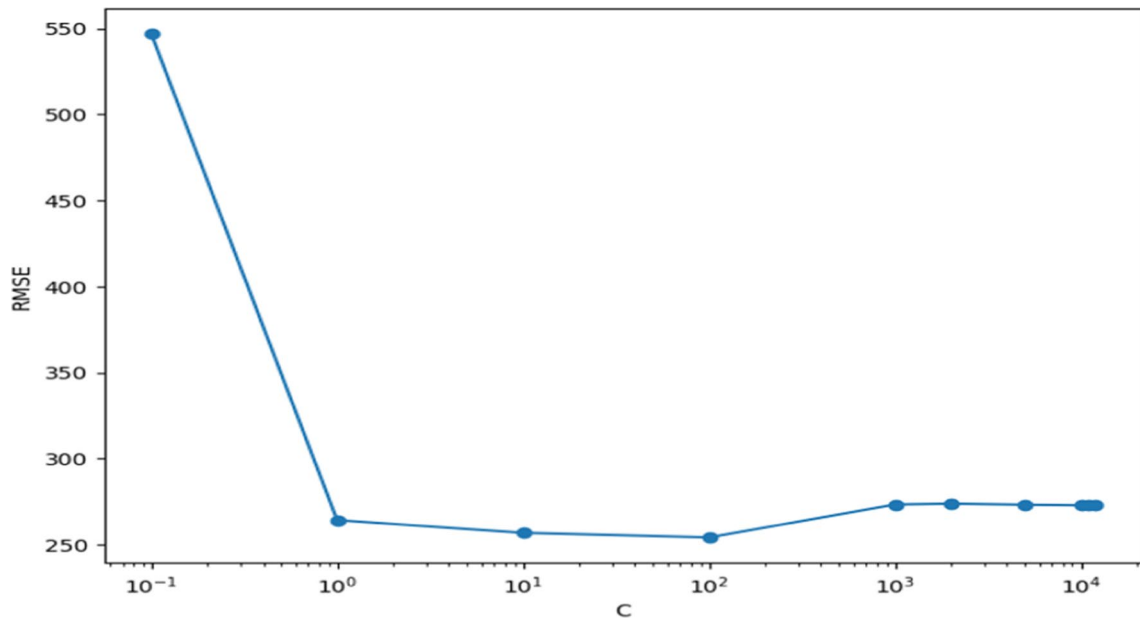
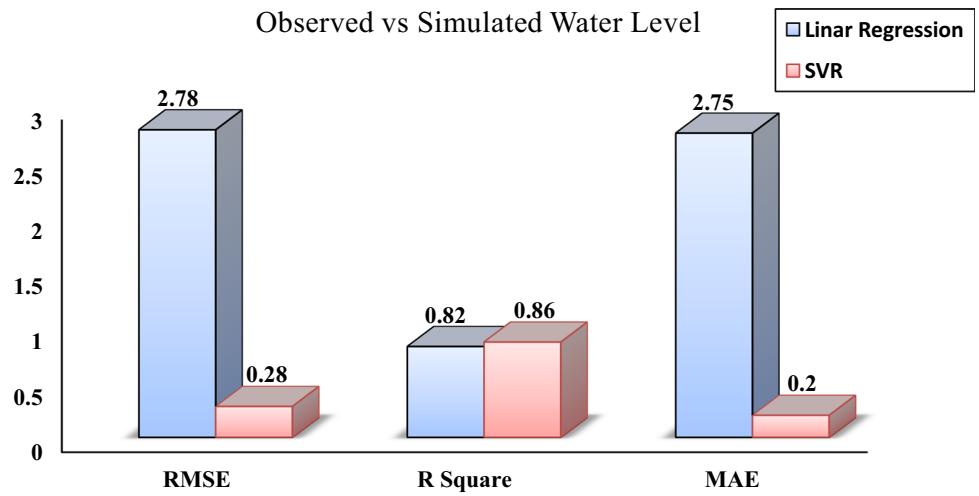


**Fig. 20** RMSE for different C values in SVR for water flow

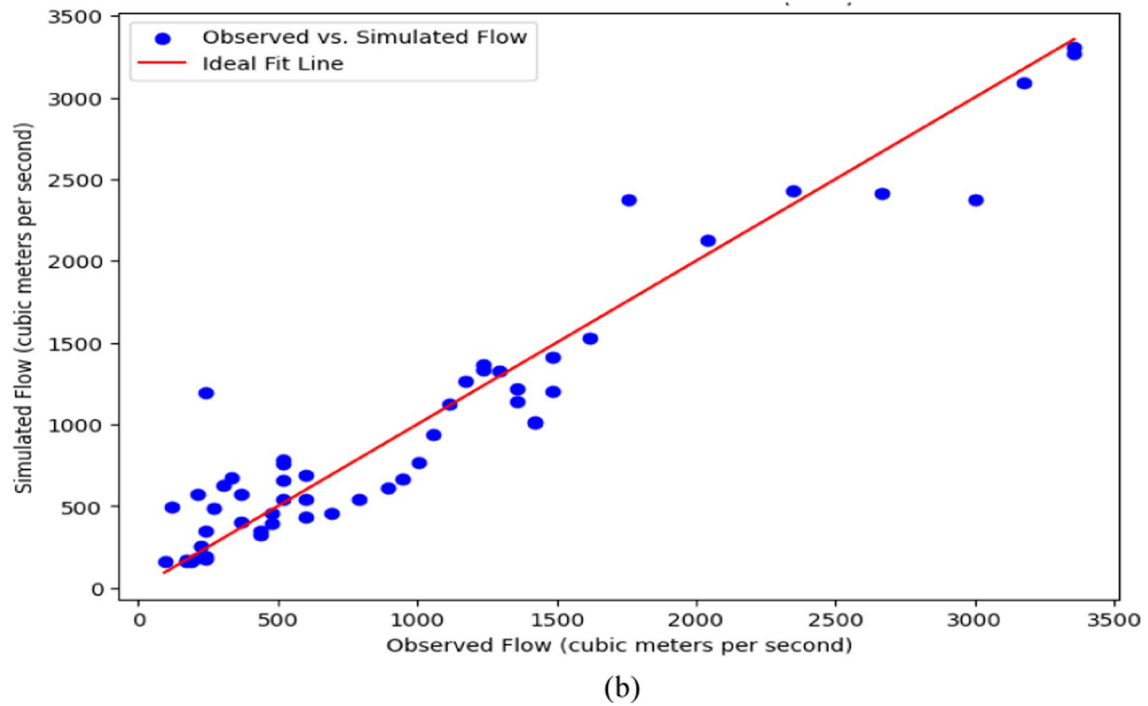
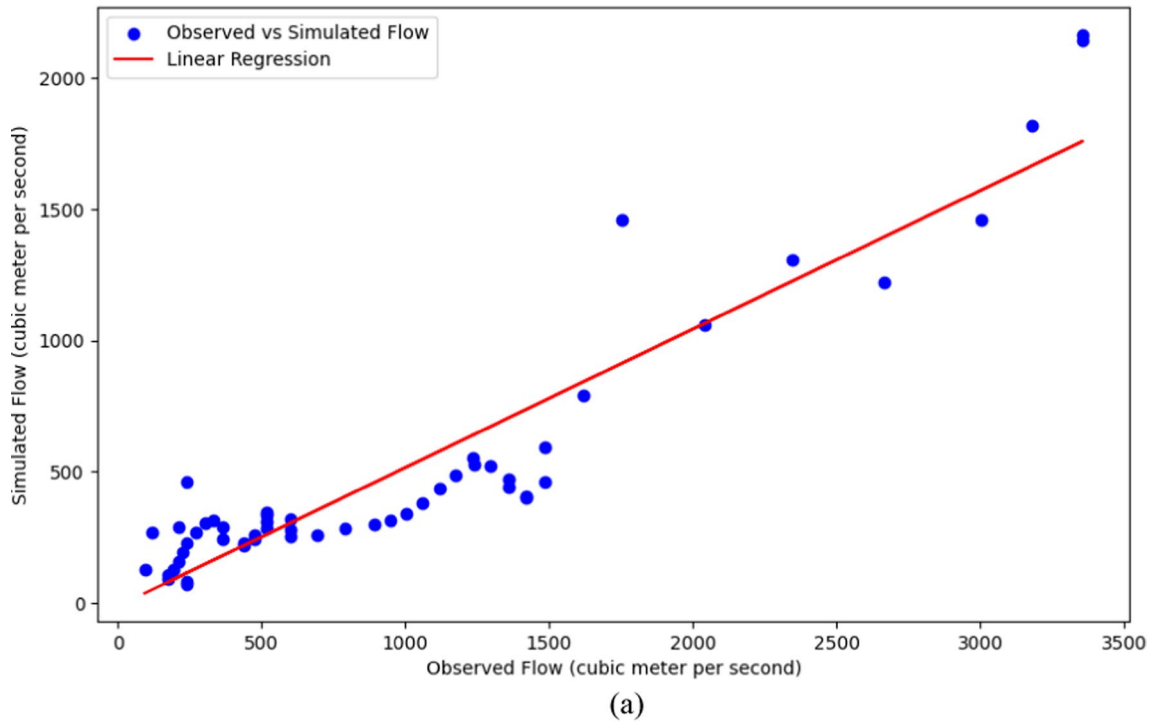
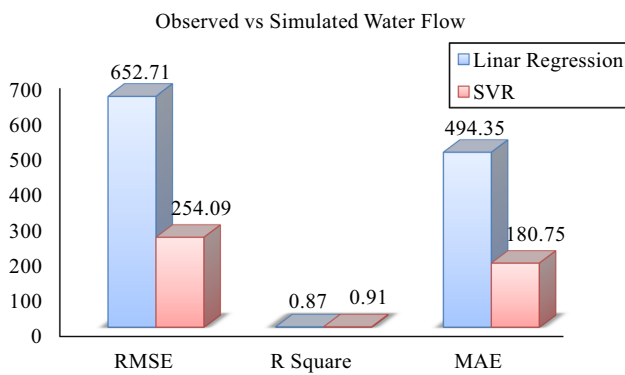


Fig. 21 Comparison of observed and simulated water flow at Dhanera bridge gauge station using **a** linear regression, **b** SVR



**Fig. 22** Model performance of observed and simulated water flow using linear regression and SVR

## Conclusion

An integrated novel approach to hydrodynamic modeling of dam breach floods, incorporating satellite imagery, Unmanned Aerial Vehicles (UAVs), and Google Earth Engine (GEE), holds significant promise for enhancing the capability to forecast downstream inundation scenarios, especially in data-scarce regions. The findings of this study underscore the high accuracy and potential real-world applicability of the proposed approach, laying the foundation for its integration into flood risk assessment and management practices.

The utilization of DJI Phantom 4 Pro and Pix4D Mapper technology in the UAVs survey demonstrated its efficacy in providing high-resolution DEMs for urban areas, facilitating precise flood modeling and mitigation planning efforts. Additionally, the integration of NASA Global Precipitation Measurement (GPM) data has proven invaluable in obtaining rainfall information for runoff studies, particularly in regions where data scarcity poses a challenge.

Furthermore, the employment of 2D HEC-RAS-based hydrodynamic modeling has empowered decision-makers to simulate floods in a two-dimensional space, enabling the creation of decision-making maps encompassing critical parameters such as water surface height, flood inundation extent, and flood velocity. These maps serve as indispensable tools for comprehensive flood risk assessment and management strategies.

In conclusion, this study underscores the pressing need to integrate advanced modeling approaches into flood management practices, not only for dam breach events but also for natural floods. By utilizing an integrated approach that incorporates satellite data, Unmanned Aerial Vehicles (UAVs), and Google Earth Engine (GEE), we can develop

more resilient and adaptive flood mitigation strategies to address the increasingly complex and unpredictable hydrological challenges we face. It is essential to emphasize that this study focused on a single dam, limiting the generalizability of the findings. Future research should aim to expand the scope to encompass multiple dams and diverse geographical settings to further refine and validate the proposed approach. Continued research efforts and collaboration are imperative to enhance our collective capacity to safeguard communities from the devastating impacts of flooding and ensure sustainable flood management practices in the face of climate change.

**Author contributions** Kishanlal Darji helped in data collection and analysis, writing, figure preparation, table creation; Dhruvesh P. Patel was involved in conceptualization, supervision, analysis, writing; Indra Prakash contributed to drafting, editing, technical reviewing, and coordinating; Hamad Ahmed Altuwajri helped in writing, technical discussion, editing.

**Funding** The authors extend their appreciation to the Researchers Supporting Project number (RSPD2024R848), King Saud University, Riyadh, Saudi Arabia. The authors are also thankful to PDPU for providing research facilities for completing this project.

**Data availability** Not applicable.

## Declarations

**Conflict of interest** The authors declare that they have no conflict of interest in this work.

**Ethical approval** We declare herein that our paper is original and unpublished elsewhere and that this manuscript complies to the Ethical Rules applicable for this journal.

**Consent to participate** All of the authors consent to participate in this research work.

**Consent for publication** All of the authors consent to publish this work.

**Open Access** This article is licensed under a Creative Commons Attribution-NonCommercial-NoDerivatives 4.0 International License, which permits any non-commercial use, sharing, distribution and reproduction in any medium or format, as long as you give appropriate credit to the original author(s) and the source, provide a link to the Creative Commons licence, and indicate if you modified the licensed material. You do not have permission under this licence to share adapted material derived from this article or parts of it. The images or other third party material in this article are included in the article's Creative Commons licence, unless indicated otherwise in a credit line to the material. If material is not included in the article's Creative Commons licence and your intended use is not permitted by statutory regulation or exceeds the permitted use, you will need to obtain permission directly from the copyright holder. To view a copy of this licence, visit <http://creativecommons.org/licenses/by-nc-nd/4.0/>.

## References

- Abdelkarim A, Gaber AFD, Alkadi II, Alogayell HM (2019) Integrating remote sensing and hydrologic modeling to assess the impact of land-use changes on the increase of flood risk: a case study of the Riyadh-Dammam train track, Saudi Arabia. *Sustainability* 11:6003. <https://doi.org/10.3390/SU11216003>
- Abdessamed D, Abderrazak B (2019) Coupling HEC-RAS and HEC-HMS in rainfall–runoff modeling and evaluating floodplain inundation maps in arid environments: case study of Ain Sefra city, Ksour Mountain SW of Algeria. *Environ Earth Sci* 78:1–17. <https://doi.org/10.1007/S12665-019-8604-6>
- Acuña P, Pizarro A (2023) Can continuous simulation be used as an alternative for flood regionalisation? A large sample example from Chile. *J Hydrol* 626:130118. <https://doi.org/10.1016/J.JHYDROL.2023.130118>
- Berghout A, Meddi M (2016) Sediment transport modeling in Wadi chemora during flood flow events. *J Water Land Dev* 31:23–31. <https://doi.org/10.1515/JWLD-2016-0033>
- Borah SB, Sivasankar T, Ramya MNS, Raju PLN (2018) Flood inundation mapping and monitoring in Kaziranga National Park, Assam using sentinel-1 SAR data. *Environ Monit Assess* 190:1–11. <https://doi.org/10.1007/S10661-018-6893-Y/FIGURES/6>
- Boussekine M, Djemili L (2016) Modelling approach for gravity dam break analysis. *J Water L Dev* 30:29–34. <https://doi.org/10.1515/JWLD-2016-0018>
- Bout B, Jetten VG (2018) The validity of flow approximations when simulating catchment-integrated flash floods. *J Hydrol* 556:674–688. <https://doi.org/10.1016/j.jhydrol.2017.11.033>
- Cronshey R, Roberts R, Miller N (1985) *Urban hydrology for small watersheds (TR-55 Rev.)*. Hydraul Hydrol
- Darji K, Patel D (2024) A dam break analysis using HEC-RAS 2D hydrodynamic modeling for decision-making system. In: Timbadiya PV, Patel Prem Lal, Singh Vijay P, Manekar Vivek L (eds) *Flood forecasting and hydraulic structures*. Springer Nature Singapore, Singapore, pp 183–194. [https://doi.org/10.1007/978-981-99-1890-4\\_14](https://doi.org/10.1007/978-981-99-1890-4_14)
- Darji K, Patel D, Dubey AK et al (2021) An approach of satellite and UAS based mosaicked DEM for hydrodynamic modelling—a case of flood assessment of Dhanera city, Gujarat, India. *J Geomat* 15:247–257
- Darji K, Patel D, Prakash I (2021b) Application of SCS-CN Method and HEC HMS Model in the Estimation of Runoff of Machhu River Basin, Gujarat, India. In: *Hydro 2020 international conference*. pp 305–316
- Darji K, Patel D, Prakash I (2022) Comparison of HEC-HMS and SWAT hydrological models in simulating runoff at Machhu river catchment, Gujarat, India. *Advanced modelling and innovations in water resources engineering*. Springer, Singapore, pp 141–156
- Darji K, Patel D, Vakharia V et al (2023) Watershed prioritization and decision-making based on weighted sum analysis, feature ranking, and machine learning techniques. *Arab J Geosci* 16:1–20. <https://doi.org/10.1007/S12517-022-11054-W>
- Darji KR, Vyas UH, Patel D, Dewals B (2024) A dam break analysis of damanganga dam using HEC-RAS 2D hydrodynamic modelling and geospatial techniques. [https://doi.org/10.1007/978-981-99-3557-4\\_1/COVER](https://doi.org/10.1007/978-981-99-3557-4_1/COVER)
- Derdous O, Djemili L, Bouchehed H, Tachi SE (2015) A GIS based approach for the prediction of the dam break flood hazard—a case study of Zardezas reservoir “skikda, Algeria.” *J Water L Dev* 27:15–20. <https://doi.org/10.1515/JWLD-2015-0020>
- Desta HB, Belayneh MZ (2020) Dam breach analysis: a case of Gidabo dam, Southern Ethiopia. *Int J Environ Sci Technol* 181(18):107–122. <https://doi.org/10.1007/S13762-020-03008-0>
- Dhiman S, Patra KC (2019) Studies of dam disaster in India and equations for breach parameter. *Nat Hazards* 98:783–807. <https://doi.org/10.1007/S11069-019-03731-Z/TABLES/11>
- do Lago CAF, Giacomoni MH, Bentivoglio R et al (2023) Generalizing rapid flood predictions to unseen urban catchments with conditional generative adversarial networks. *J Hydrol* 618:129276. <https://doi.org/10.1016/J.JHYDROL.2023.129276>
- Elfeki A, Masoud M, Niyazi B (2016) Integrated rainfall–runoff and flood inundation modeling for flash flood risk assessment under data scarcity in arid regions: Wadi Fatimah basin case study, Saudi Arabia. *Nat Hazards* 85:87–109. <https://doi.org/10.1007/S11069-016-2559-7>
- Flood Risk Discussion Paper (2019) International Actuarial Association Actuarielle Internationale
- Gallegos HA, Schubert JE, Sanders BF (2009) Two-dimensional, high-resolution modeling of urban dam-break flooding: a case study of Baldwin Hills, California. *Adv Water Resour* 32:1323–1335. <https://doi.org/10.1016/J.ADVWATRES.2009.05.008>
- Jha MK, Afreen S (2020) Flooding urban landscapes: Analysis using combined hydrodynamic and hydrologic modeling approaches. *Water (Switzerland)*. <https://doi.org/10.3390/w12071986>
- Juliausti SO (2017) Dam break analysis and flood inundation map of Krisak dam for emergency action plan. *AIP Conf Proc* 1903:100005. <https://doi.org/10.1063/1.5011615>
- Khan MS, Coulibaly P (2006) Application of support vector machine in lake water level prediction. *J Hydrol Eng* 11:199–205. [https://doi.org/10.1061/\(ASCE\)1084-0699\(2006\)11:3\(199\)/ASSET/33BE6F38-BC0B-48AD-950A-E3F89B1D007D/ASSETS/IMAGES/6.JPG](https://doi.org/10.1061/(ASCE)1084-0699(2006)11:3(199)/ASSET/33BE6F38-BC0B-48AD-950A-E3F89B1D007D/ASSETS/IMAGES/6.JPG)
- Lastra J, Fernández E, Díez-Herrero A, Marquín J (2008) Flood hazard delineation combining geomorphological and hydrological methods: an example in the Northern Iberian Peninsula. *Nat Hazards* 45:277–293. <https://doi.org/10.1007/S11069-007-9164-8>
- Liu X, Yang S, Ye T et al (2021) A new approach to estimating flood-affected populations by combining mobility patterns with multi-source data: a case study of Wuhan, China. *Int J Disaster Risk Reduct*. <https://doi.org/10.1016/J.IJDRR.2021.102106>
- Matgen P, Schumann G, Henry JB et al (2007) Integration of SAR-derived river inundation areas, high-precision topographic data and a river flow model toward near real-time flood management. *Int J Appl Earth Obs Geoinf* 9:247–263. <https://doi.org/10.1016/J.JAG.2006.03.003>
- Mosavi A, Ozturk P, Chau KW (2018) Flood prediction using machine learning models: literature review. *Water (switzerland)* 10:1–40. <https://doi.org/10.3390/w10111536>
- Naeem B, Azmat M, Tao H et al (2021) Flood hazard assessment for the tori levee breach of the indus river basin, Pakistan. *Water (switzerland)* 13:1–19. <https://doi.org/10.3390/w13050604>
- Pandya PH, Thakor DJ (2013) A brief review of method available for dam break analysis. *Paripex-Indian J Res* 2:41–3. <https://doi.org/10.36106/PARIPEX>
- Patel D, Darji KR, Dubey AK, et al (2024) Application of open-source geospatial and modeling techniques for flood assessment and management—a case of flood 2017, Rel River catchment. pp 51–61. [https://doi.org/10.1007/978-981-99-3557-4\\_5/COVER](https://doi.org/10.1007/978-981-99-3557-4_5/COVER)
- Patel DP, Pandya UD (2021) Flood stages assessment using open source 1D hydrodynamic modelling in data scarce region. *Int J Hydrol Sci Technol* 1:1. <https://doi.org/10.1504/IJHST.2021.10039735>
- Patel DP, Ramirez JA, Srivastava PK et al (2017) Assessment of flood inundation mapping of Surat city by coupled 1D/2D hydrodynamic modeling: a case application of the new HEC-RAS 5. *Nat Hazards* 89:93–130. <https://doi.org/10.1007/S11069-017-2956-6>
- Pathan A, Kantamaneni K, Agnihotri P et al (2022a) Integrated flood risk management approach using mesh grid stability and



- hydrodynamic model. *Sustainability* 14:16401. <https://doi.org/10.3390/SU142416401>
- Pathan AI, Agnihotri PG, Patel D (2022b) Prieto C (2022b) Mesh grid stability and its impact on flood inundation through (2D) hydrodynamic HEC-RAS model with special use of Big Data platform—a study on Purna River of Navsari city. *Arab J Geosci* 157(15):1–23. <https://doi.org/10.1007/S12517-022-09813-W>
- Pradhan P, Tingsanchali T, Shrestha S (2020) Evaluation of soil and water assessment tool and artificial neural network models for hydrologic simulation in different climatic regions of Asia. *Sci Total Environ* 701:134308. <https://doi.org/10.1016/J.SCITOTENV.2019.134308>
- Quiroga VM, Kurea S, Udo K, Manoa A (2016) Application of 2D numerical simulation for the analysis of the February 2014 Bolivian Amazonia flood: application of the new HEC-RAS version 5. *Ribagua* 3:25–33. <https://doi.org/10.1016/j.riba.2015.12.001>
- Rezaeianzadeh M, Tabari H, Arabi Yazdi A et al (2014) Flood flow forecasting using ANN, ANFIS and regression models. *Neural Comput Appl* 25:25–37. <https://doi.org/10.1007/S00521-013-1443-6/METRICS>
- Sahoo SN, Sreeja P (2017) Development of flood inundation maps and quantification of flood risk in an urban catchment of Brahmaputra River. *ASCE-ASME J Risk Uncertain Eng Syst Part A Civ Eng* 3:1–11. <https://doi.org/10.1061/ajrua6.0000822>
- Singh NK, Yadav M, Singh V et al (2023) Artificial intelligence and machine learning-based monitoring and design of biological wastewater treatment systems. *Bioresour Technol* 369:128486. <https://doi.org/10.1016/J.BIORTECH.2022.128486>
- Subramanya K (2013) *Engineering Hydrology* 4th Ed., McGraw Hill Education India. [https://www.google.com/search?xsrf=ALiCsYtsXhaVHHTrnYh32GCQgerytex\\_g:1658394538305&q=Engineering+Hydrology&stick=H4sIAAAAAAAAAAONgVeLR T9c3NCorM8tINjE1EvRWKC5NKkrMTcyrTFRIys\\_PPswIouUIy-Ia5hUWWReYmJejuDnWVaaWxrA-GkG5SUIBIU5pxi59HP1Dcyy8qN4mFmJeUZFBumw-Xy](https://www.google.com/search?xsrf=ALiCsYtsXhaVHHTrnYh32GCQgerytex_g:1658394538305&q=Engineering+Hydrology&stick=H4sIAAAAAAAAAAONgVeLR T9c3NCorM8tINjE1EvRWKC5NKkrMTcyrTFRIys_PPswIouUIy-Ia5hUWWReYmJejuDnWVaaWxrA-GkG5SUIBIU5pxi59HP1Dcyy8qN4mFmJeUZFBumw-Xy). Accessed 21 Jul 2022
- Trambadia NK, Patel DP, Patel VM, Gundalia MJ (2022) Comparison of two open-source digital elevation models for 1D hydrodynamic flow analysis: a case of Ozat River basin, Gujarat, India. *Model Earth Syst Environ* 8:5433–5447. <https://doi.org/10.1007/S40808-022-01426-2/METRICS>
- Vojtek M, Vojteková J (2016) Flood hazard and flood risk assessment at the local spatial scale: a case study. *Geomat, Nat Hazards Risk* 7:1973–1992. <https://doi.org/10.1080/19475705.2016.1166874>
- Wang B, Chen Y, Wu C et al (2016) A semi-analytical approach for predicting peak discharge of floods caused by embankment dam failures. *Hydrol Process* 30:3682–3691. <https://doi.org/10.1002/HYP.10896>
- Yalcin E (2019) Two-dimensional hydrodynamic modelling for urban flood risk assessment using unmanned aerial vehicle imagery: a case study of Kirsehir. *Turkey J Flood Risk Manag* 12:e12499. <https://doi.org/10.1111/jfr3.12499>
- Zagonjoli M (2007) *Dam break modelling, risk assessment and uncertainty analysis for flood mitigation*. A.A.Balkema Publisher, Delft, Netherlands
- Zhang Y, Wang Y, Chen Y et al (2019) Assessment of future flash flood inundations in coastal regions under climate change scenarios—a case study of Hadahe River basin in northeastern China. *Sci Total Environ* 693:133550. <https://doi.org/10.1016/j.scitotenv.2019.07.356>
- Zhang Y, Wang Y, Zhang Y et al (2020) Multi-scenario flash flood hazard assessment based on rainfall–runoff modeling and flood inundation modeling: a case study. *Nat Hazards* 1051(105):967–981. <https://doi.org/10.1007/S11069-020-04345-6>

**Publisher's Note** Springer Nature remains neutral with regard to jurisdictional claims in published maps and institutional affiliations.